

Santa Clara University

Scholar Commons

Bioengineering Senior Theses

Engineering Senior Theses

Spring 2021

Skin Phantom for Biowearable Device Testing

Ruby Karimjee

Brooke Fitzwilson

Jordan Spice

Follow this and additional works at: https://scholarcommons.scu.edu/bioe_senior



Part of the [Biomedical Engineering and Bioengineering Commons](#)

SANTA CLARA UNIVERSITY

Department of Bioengineering

I HEREBY RECOMMEND THAT THE THESIS PREPARED
UNDER MY SUPERVISION BY

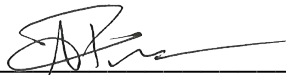
Ruby Karimjee, Brooke Fitzwilson, Jordan Spice

ENTITLED

**SKIN PHANTOM FOR
BIOWEARABLE DEVICE TESTING**

BE ACCEPTED IN PARTIAL FULFILLMENT OF THE REQUIREMENTS
FOR THE DEGREE OF

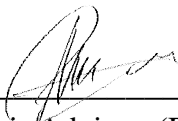
**BACHELOR OF SCIENCE
IN
BIOENGINEERING**



Thesis Advisor (Dr. Prashanth Asuri)

6/10/2021

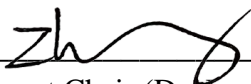
date



Thesis Advisor (Dr. Emre Araci)

6/10/2021

date



Department Chair (Dr. Jonathan Zhang)

6/10/2021

date

SKIN PHANTOM FOR BIOWEARABLE DEVICE TESTING

By

Ruby Karimjee, Brooke Fitzwilson, Jordan Spice

SENIOR DESIGN PROJECT REPORT

Submitted to
the Department of Bioengineering

of

SANTA CLARA UNIVERSITY

in Partial Fulfillment of the Requirements
for the degree of
Bachelor of Science in Bioengineering

Santa Clara, California

Spring 2021

Table of Contents

| | |
|---|-----|
| Abstract | iii |
| Acknowledgments | iv |
| List of Figures | v |
| List of Tables | vii |
| Chapter 1: Project Introduction | 1 |
| 1.1 Project Rationale | 1 |
| 1.1.1 Problems with Current Methods of Biowearable-Skin Interface Testing | 2 |
| 1.2 Physiology of Human Skin Contributing to Impedance | 3 |
| 1.3 Existing Skin Phantoms | 4 |
| 1.3.1 Textile Skin Phantoms | 5 |
| 1.3.2 Metal Skin Phantoms | 6 |
| 1.3.3 Elastomer Skin Phantoms | 6 |
| 1.3.4 Gelatinous Skin Phantoms | 7 |
| 1.4 Existing COMSOL Models | 7 |
| 1.5 Market Needs Analysis | 9 |
| Chapter 2: The Skin Phantom System | 11 |
| 2.1 System Overview | 11 |
| 2.2 Subsystem Goals | 11 |
| 2.2.1 The Physical Model Subsystem | 12 |
| 2.2.2 COMSOL Electrical Data Simulation | 12 |
| 2.2 Integration of Subsystems | 12 |
| Chapter 3: The Physical Model | 14 |
| 3.1 Overview of Subsystem | 16 |
| 3.2 Material Choice | 16 |
| 3.3 Fabrication | 15 |
| 3.3.1 Agar Layer | 16 |
| 3.3.2 Silicone Layer | 16 |
| 3.4 Electrical Data Collection | 19 |
| Chapter 4: COMSOL Simulations of the Skin Phantom | 21 |
| 4.1 Overview of Subsystem | 28 |
| 4.2 Software | 22 |
| 4.3 Parameters | 28 |
| 4.3.1 Geometry and Material | 23 |

| | |
|---|----|
| 4.3.2 Physics | 24 |
| 4.3.3 Electric Currents Module | 26 |
| 4.3.4 Frequency Domain Study | 27 |
| 4.3.5 Evaluation Expressions for Admittance | 27 |
| 4.4 Models | 28 |
| 4.4.1 Preliminary Model | 28 |
| 4.4.2 Final Model | 28 |
| 4.5 MATLAB Code | 30 |
| 4.5.1 Initial Data Preparation | 31 |
| 4.5.2 Program Function | 31 |
| Chapter 5: Results | 33 |
| 5.1 Educational Kit | 33 |
| 5.1.1 Agar Layer | 33 |
| 5.1.2 Silicone Layer | 34 |
| 5.2 COMSOL Simulation | 36 |
| 5.2.1 Sweat Pooling | 36 |
| 5.2.2 Electrode Distance | 39 |
| 5.2.3 Conductivity and Relative Permittivity | 41 |
| 5.2.4 Model Validation vs. Capacitor | 43 |
| 5.2.5 Model Validation vs. Real Skin | 45 |
| Chapter 6: Professional Engineering Standards and Realistic Constraints | 47 |
| 6.1 Ethical Justification of Skin Phantoms | 47 |
| 6.2 Health and Safety Implications | 47 |
| 6.3 Sustainability as a Constraint | 48 |
| 6.4 Civic Engagement and Compliance with Regulations | 48 |
| 6.5 Manufacturability | 49 |
| 6.6 Budget Constraints | 49 |
| 6.7 Time Constraints | 50 |
| 6.7.1 Model Constraints | 50 |
| Chapter 7: Summary and Conclusion | 52 |
| 7.1 Summary of Project Work | 52 |
| 7.2 Future Work | 52 |
| 7.2.1 Educational Kit | 52 |
| 7.2.2 COMSOL Model | 53 |
| 7.3 Lessons Learned | 53 |
| References | 54 |

| | |
|--|----|
| Appendix A: Budget and Actual Spending | 58 |
| A.1: Proposed Budget (if lab were accessible) | 58 |
| A.2: Purchase Record | 59 |
| Appendix B: Engineering 1 Lab Instruction Packet | 60 |
| Appendix C: Project Timeline | 66 |
| C.1: Original Projected Timeline | 66 |
| C.2: Actual Timeline Due to Campus Closures/Lab Access | 67 |
| Appendix D: COMSOL Equations | 68 |
| D.1: Current Conversion Equations | 68 |
| D.2: Complex Impedance for RC Circuit [31]. | 68 |
| Appendix E: MATLAB Program | 69 |
| E.1: Example Text File Export from COMSOL | 69 |
| E.2: Pseudocode | 70 |
| E.3: Example Main Script (Commented) | 71 |
| E.4: Example Local Functions (Commented) | 72 |
| E.4.1: comsolextraction() | 72 |
| E.4.2: getdata() | 73 |
| E.4.3: impedance() | 73 |

Abstract

The biowearable industry currently utilizes animals, humans, and cadavers for testing skin mounted bio-devices. There is a need for a sustainable skin phantom that is capable of simulating the properties of skin. We proposed a skin phantom educational kit that emulates the perspiration and electrical properties (i.e. impedance spectrum) of skin. This kit can mimic the effects of different sweat concentrations and geometrical structures and allows students to visualize how these properties change electrical measurements. We designed a three-layered model composed of silicone rubber sandwiched between agar, which is similar to the skin's elastomeric and porous texture. We used simple and safe equipment such as a digital multimeter and a low-voltage power source for testing our educational model.

We also constructed a computational model using COMSOL Multiphysics to simulate important skin phantom properties. Our COMSOL model is more complex than the agar-silicone layered model in the sense that it allows analysis of the impedance spectrum as a function of the perspiration mechanics. Through our COMSOL model, we achieved simulation of perspiration and studies on the effects of electrode distance, and material conductivity and relative permittivity in relation to impedance. From these tests, the simulation proves viable for scaling up to a realistic size, as our final model is sized-down for improved model development and testing purposes. Our COMSOL model serves as the groundwork for future improvements on replicating the skin's mechanical, fluid, and electrical properties in a computer simulation.

Acknowledgments

We would like to thank the following individuals for making this project possible:

1. Our advisors **Dr. Asuri** and **Dr. Araci** for their guidance and mentorship in both our physical model and COMSOL simulation. Their feedback was instrumental in translating our ideas into tangible success.
2. **Ju Young Lee** and **Kiran Sutaria**, whose previous Senior Design work inspired our design.
3. **Matthew Blanco**, who shipped us materials that we needed in an extremely efficient manner despite ongoing circumstances.
4. Our **housemates** for allowing us to run experiments at home amidst a pandemic.
5. Our **families** for their love and support throughout our undergraduate careers.

List of Figures

| | |
|---|----|
| Figure 1.1: Popular everyday-use biowearable devices..... | 1 |
| Figure 1.2: Impedance vs. frequency plot from Proteus Digital Health | 4 |
| Figure 1.3: Existing skin models and the properties they are able to mimic | 5 |
| Figure 1.4: Geometry of sweat gland model from University of Southampton | 8 |
| Figure 1.5: Geometry of capacitor from COMSOL library | 9 |
| Figure 1.6: Target customer needs for biowearable device companies..... | 10 |
| Figure 2.1: Systems level diagram of skin phantom testing..... | 11 |
| Figure 3.1: Systems level flowchart of inputs and outputs in physical model | 14 |
| Figure 3.2: Skin phantom assembly with porous silicone and 4% Agar | 15 |
| Figure 3.3: Making the agar gel..... | 16 |
| Figure 3.4: Creating the silicone molds | 17 |
| Figure 3.5: Enhancing porous silicone with salt..... | 17 |
| Figure 3.6: Simulating epidermis with Transpore Surgical Tape | 18 |
| Figure 3.7: Setting up the educational kit circuit..... | 19 |
| Figure 3.8: Electrode configuration for gel model | 19 |
| Figure 4.1: Resistor and capacitor in series | 23 |
| Figure 4.2: Resistance equation..... | 23 |
| Figure 4.3: Capacitance equation..... | 23 |
| Figure 4.4: Impedance of CPE capacitor equation | 24 |
| Figure 4.5: Relationship between impedance and admittance..... | 24 |
| Figure 4.6: Preliminary COMSOL epidermis model..... | 27 |
| Figure 4.7: Isometric view of final COMSOL epidermis model..... | 28 |
| Figure 4.8: Further views of the final epidermis model | 28 |
| Figure 4.9: Systems level flowchart of COMSOL-to-MATLAB pipeline | 29 |
| Figure 5.1: Resistance vs. NaCl concentration in 4% Agar of varying thicknesses..... | 32 |
| Figure 5.2: Current vs. NaCl concentration in 4% Agar of varying thicknesses..... | 32 |
| Figure 5.3: Porous silicone made with 1 g sugar in 15 mL silicone..... | 34 |
| Figure 5.4: COMSOL diagrams in isometric view | 36 |
| Figure 5.5: Impedance vs. frequency for varying surface sweat pooling radii..... | 38 |
| Figure 5.6: COMSOL top-down view of electrode distances | 39 |

Figure 5.7: Impedance vs. frequency for varying electrode distances.....39
Figure 5.8: Impedance vs. frequency using sweat property values41
Figure 5.9: Impedance vs. frequency using epidermis property values.....42
Figure 5.10: Capacitor model using epidermis property values43
Figure 5.11: Impedance vs. frequency graphs with correlating models44
Figure 5.12: Impedance vs. frequency from *in vivo* and our model45

List of Tables

| | |
|--|----|
| Table 4.3: Parameter names and values in COMSOL | 22 |
| Table 4.4: Conductivity and relative permittivity values for model features | 25 |
| Table 5.1: Current flow for silicone layers on top of 4% Agar with 1% NaCl..... | 35 |
| Table 5.2: Correlating height and radius combinations tested for sweat pooling..... | 37 |

Chapter 1: Project Introduction

1.1 Project Rationale

Our world is currently seeing an overall transformation in the healthcare system to being centered on the individual. With that, wearable sensors are becoming widespread in healthcare due to their ability to provide real-time feedback while being non-invasive. While the more well-known biowearables might be devices such as the Fitbit or Apple Watch, shown in Figure 1.1, the biowearables field is expansive and includes technologies such as smart contact lenses, glucose sensors, and even electronic tattoos. These biowearables have the potential to improve the way we treat many diseases, but a limiting factor is the extensive testing phase. The effect of the device on the skin must be known and quantified before it goes to market. However, most of the tests have been *in vitro* or *in vivo* methods, which not only have ethical concerns but can also be inaccurate. There has only recently been a shift toward synthetic materials, or skin phantoms, which would emulate the desired properties of human skin.



Figure 1.1: Popular everyday-use biowearable devices. The Fitbit and Apple Watch [1].

This project is a continuation of a 2019-2020 Santa Clara University Bioengineering team that was working with a company called Proteus Digital Health [2]. The goal of the company was to optimize a biometric patch, worn on the abdomen, to monitor ingested medicines and capture the physiologic response. They expressed the need for a skin phantom to use for early-stage testing of their device; thus, began the skin phantom senior design project with

the objective of creating a skin phantom capable of accurately replicating the electrical properties and behaviors of real skin. The other portion of our project is a more simple educational kit, which would allow students of various ages to learn about factors that impact the conductivity of the skin.

1.1.1 Problems with Current Methods of Biowearable-Skin Interface Testing

There are currently two main methods used in the testing biowearables. The first is *in vivo* through testing on animals and humans. Regulatory bodies typically make recommendations or requirements or set minimum performance criteria for these to be used. While there are commercial manufacturers who can manufacture them in an affordable manner, their development can be inconsistent [3]. This makes it difficult to share research or even rely on these methods as a predictor for how the device will function. When testing on humans, they must also be screened to meet eligibility criteria, and there are more ethical considerations, such as informed consent and patient history.

While there may be variation between individuals, the physiological and anatomical differences between humans and animals lead to far more misleading results. Skin barriers vary among species due to the amount of free fatty acids and triglycerides, as well as the density of hair follicles. Studies have shown a lack of correlation in transdermal drug permeation among species and even in different sites within a single animal due to variations in skin thickness, the presence of skin shafts, and the composition of lipids [4].

The second main method is *in vitro*, which would involve cadavers. While they may be more accurate than animals in terms of anatomy and physiology, there is still the issue of individual to individual variation. There are also very few available, so they can be expensive due to their cost of transportation, embalming, and storage. Finally, cadavers also raise large ethical dilemmas about whether biospecimens are considered human subjects and are therefore held to standards of informed consent [5]. Because of this, they are subject to extensive state and federal regulations. With so few available, cadavers would have more value in practicing medical procedures and shouldn't be relied on to routinely test biowearables.

1.2 Physiology of Human Skin Contributing to Impedance

Before designing both our physical model and COMSOL simulation, we consolidated literature research on skin physiology. This would help us determine which factors we should incorporate into our subsystems. Proteus Digital Health wanted a patch that would mimic the abdomen but since we are not working with the company, we decided to keep our site options open. We found that abdomen perspiration is very similar to that of the forearm, an area for which many biowearables are innovated, so we focused our research on this site [6].

The water content and sweat properties of the skin determine its impedance values, so the better hydrated the skin is, the more water and sweat present, and the lower the skin's impedance values [7], [8]. Most of the variability in steady-state sweat rate between individuals is due to differences in sweat secretion rate per gland, rather than the number of active sweat glands. The sweat rate can be calculated by multiplying the sweat gland density by the secretion rate per gland. At rest, this rate would be $\sim 397.8 \text{ ug/cm}^2/\text{min}$, while exercising this rate can be $\sim 826.2 \text{ ug/cm}^2/\text{min}$ [9], [10]. This is an enormous difference in perspiration rates and consequent output volume of sweat; thus, biowearable devices which are not tested on perspiring individuals may be highly inaccurate. Hydration and sweat can decrease impedance and therefore alter any electrical activity that is being measured.

While ethnicity is more likely to affect optical measurements, there is a chance that it can affect electrical measurements. One study looked at the density and size of facial skin pores across women of different ethnicities [11]. Age had a nonsignificant impact, but Chinese women had significantly lower pore densities and Indian women had significantly higher pore densities. This is likely due to differences in sun exposure and lifestyle, but additional studies should be done on whether this effect can be similarly seen in other areas of the body, so biowearable devices can be made more inclusive and accurate to all races and genders.

Perspiration rates, skin hydration levels, and sweat chemical makeup will vary depending on the person, therefore indicating that the impedance of human skin varies greatly from person to person. Thus, emphasizing the importance of developing a skin phantom with easily

adaptable characteristics to account for the high variability of skin impedance [9]. One of the employees at Proteus Digital Health graciously provided *in vivo* impedance vs. frequency data using his own skin (Fig. 1.2) -- this has been the “gold standard” behavior that we try to achieve with our simulations. Since impedance vs. frequency values may differ largely from person to person, the goal of our model is to see that it largely maintains the same *behavior* as real skin measurements, as opposed to the same magnitude.

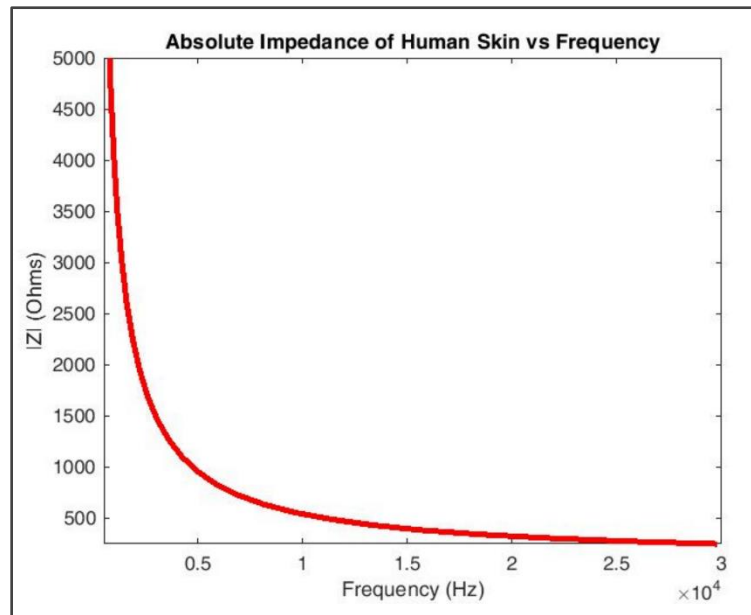


Figure 1.2: *In vivo* human skin impedance vs. frequency data from Proteus Digital Health’s employee, Jim Hutchinson [2].

1.3 Existing Skin Phantoms

Although rather simplistic, there have been several notable developments in skin phantoms’ design and experimentation. Figure 1.3 illustrates the major classes of those which exist and the properties that they can emulate. Overall, there are models using liquid suspension, gelatinous substances, elastomers, epoxy resin, metals, and textiles. We chose to focus on textiles, metals, elastomers, and gelatinous substances for our research because we want our model to address optimal sweating and electrical conductivity for biowearables testing. Textiles, metals, and elastomers address either of those qualities, but gelatinous substances do not. Although gelatinous substances do not have the specific properties we want, they exist for almost every other property in the figure and we believed the potential combination

of the materials could produce our desired effects. Ultimately, we decided on a gelatinous layer for conductivity, paired with an elastomer for viscoelasticity.

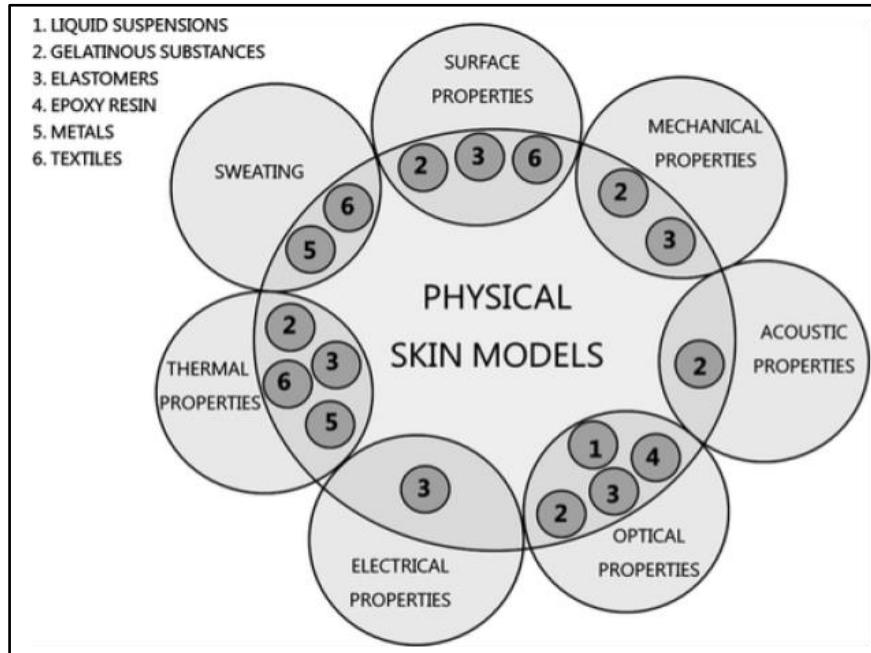


Figure 1.3: Illustrative diagram of the existing skin models and the properties they are able to mimic. Top left corner lists the types of skin models, numbered for use in the diagram. [12]

1.3.1 Textile Skin Phantoms

Textile skin phantoms have the goal of clothing-based biowearable devices. The textile material can be composed of natural or synthetic materials such as cotton, leather, polyester, and chamois. One of the features textiles-based skin phantoms look at simulating is sweat distribution due to the fiber of the textile material being porous. For sweat simulation, there are three main types of textiles. There are pre-wetter textile skins, textile skins with water delivered through sweating nozzles, and waterproof textiles that are also permeable. All three of these can be used to investigate liquid-vapor transport of skin synthetically. An application is using water distribution in textiles using X-ray micro-computed tomography [12].

1.3.2 Metal Skin Phantoms

Metal skin phantoms are primarily made for their sweating and thermal properties. The advantages to having a metal phantom are the high thermal responsiveness, the material's stable properties, and robustness [12]. An example is a porous sintered metal plate that is heated to 35°C as a sweating guarded-hotplate. This can then assess textile-physiological effects in steady-state conditions and simulate evaporating sweat coming into contact with the textile [12]. By making the metal porous, the material becomes a suitable candidate to test sweating applications. An example of a metal phantom, is one that utilized the combination of PDMS and nickel, Ni [13]. The metal phantom had the properties of flexibility similar to skin from the PDMS, but the electrical properties from the nickel to create a candidate for robotic tactile sensor applications [13]. For metal skin phantoms, the fabrication process is usually time intensive with the need of specialized equipment for processes such as hot embossing or photolithography.

1.3.3 Elastomer Skin Phantoms

Elastomers are a wide range of polymers that are rubber-like, and have many mechanical properties that are similar to that of skin. Elastomers can be natural or synthetic such as silicones and polyurethane which are most commonly used to represent the skin [12]. Elastomers are mostly used for surface property applications but are also used in electrical, mechanical, and optical. An example of an elastomer skin phantom is the silicone models used for training medical students. The silicone has similar mechanical properties as the skin making it ideal to practice surgical procedures such as stitching. Another use of silicone skin phantom is for apprenticing tattoo artists. Silicone as an elastomer, has similar optical properties as human skin making it also ideal for people training in the tattoo industry to practice on a skin phantom that reacts and feels similarly to real skin.

In an existing skin phantom, Silflo replica resin was used to place onto real human skin and then peel off creating an inverse print of the skin to best replicate the skin texture [14]. This skin phantom was utilized for surface properties and perspiration, avoiding the need for complicated manufacturing procedures such as photolithography. Another common elastomer used for skin phantoms is polydimethylsiloxane or PDMS. Last year's design team

utilized PDMS for the lab skin phantom. Other skin phantoms utilized PDMS with polyvinyl alcohol, PVA, “hydrogel cross-linked with Glutaraldehyde, GA” [15]. This combination allowed a creation of a mechanical property focused, epidermal skin equivalent [15].

1.3.4 Gelatinous Skin Phantoms

Gelatinous skin phantoms have the ability to interact with water leading to the reversible creation of gels. This allows modification and controlling of various mechanical, chemical, and physical properties such as elastic modulus, hardness, optical, and surface properties to best resemble skin. This stems from their ability to be influenced by factors such as pressure, pH and temperature [12].

There are multiple types of materials that are gelatinous, such as: gelatine, agar, agarose, collagens, and polyvinyl alcohol gels. Gelatines are typically used in testing adhesives, but they also have a density, sound speed, and adsorption/light scattering, similar to that of human skin [12]. This makes these materials ideal for mechanical and optical applications. One promising phantom made of electrical applications utilized a cuboid gelatine phantom with Ag/AgCl electrodes, but it did not mimic perspiration [16]. Agar and agarose are similar to gelatine, and they can have their electrical properties manipulated by adding NaCl to control the conductivity. However, the agar and agarose in this aspect are limited to non-contact applications [12].

1.4 Existing COMSOL Models

Skin models in COMSOL are few and far between. However, a 2018 thesis paper called “A Cellular Model of the Electrical Characteristics of Skin” from the University of Southampton proved to be incredibly useful for determining how to set up a COMSOL simulation for skin [17]. In the thesis, the author goes over multiple iterations of differing models for skin -- the model that was most useful to our project is shown in Figure 1.3. Their thesis is concerned primarily with the effect of hydration and electroporation on skin impedance when electrical stimulation signals are applied. They looked at the impedance vs. conductivity behaviors in a cellular setting and how frequency plays a role in that relationship.

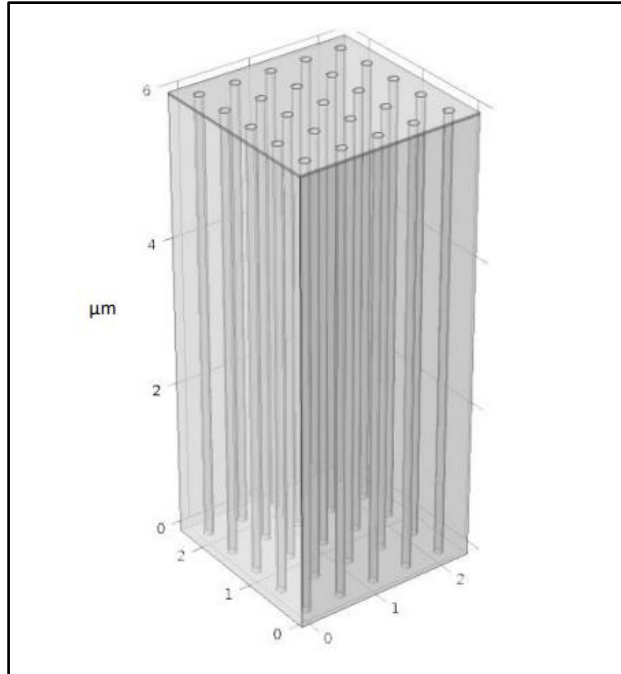


Figure 1.4: Geometry of sweat gland model from University of Southampton [17]. The model features a thin layer of stratum corneum on top of epidermis with sweat glands.

The Figure 1.3 model was what we wanted to be able to achieve, but we wanted to do so on a much smaller scale. Instead, we implemented only one layer being the stratum corneum. This COMSOL model focused on the impedance vs. conductivity of the skin, while we are focusing on the impedance vs. frequency [17]. Their paper also had the values of the relative permittivity and conductivity for the sweat and stratum corneum which we utilized for our baseline values within our COMSOL model.

To understand how the Electric Currents physics module works in COMSOL, we utilized the COMSOL website resources where they had a completed capacitor model that included the Electric Currents physics module (Fig. 1.4) [18]. This capacitor model features contraplanar electrodes, meaning the electrodes are on opposite sides of the model, and its only materials are air and glass. Air and glass are hardly materials replicative of human skin and this model does not have any pores or coplanar electrodes as our final design would require. Despite these differences, this capacitor model helped us better understand how to set up some of the Electric Currents physics in COMSOL as it was valuable to be able to search through their model's physics parameters and COMSOL Study set up.

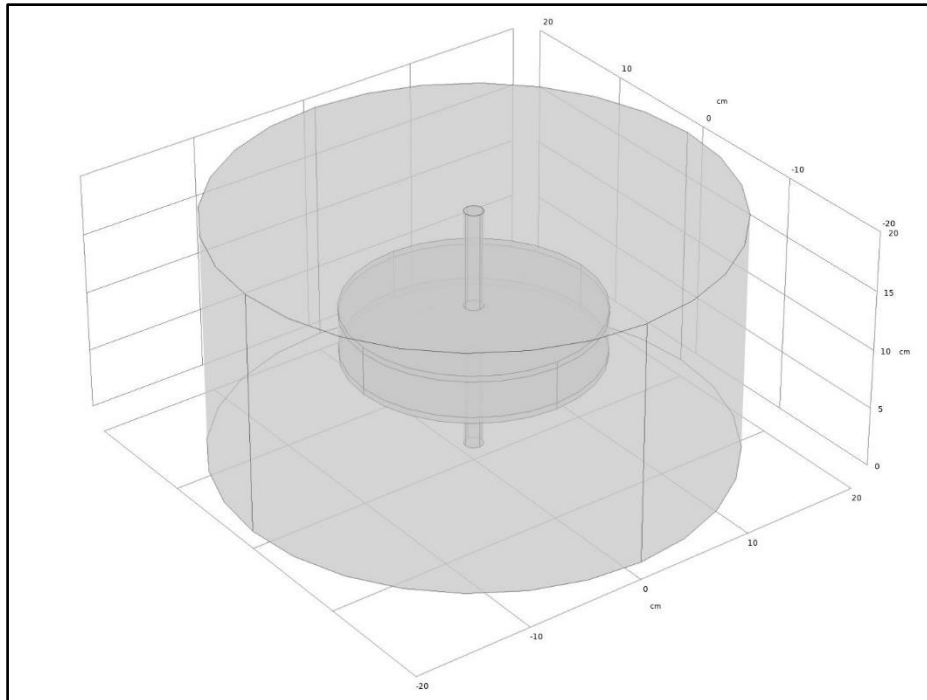


Figure 1.5: Geometry of capacitor from COMSOL library [18]. The model is composed of only glass and air. The very middle cylindrical disc is made of glass and everything else is made of air. The thin cylinders stacked on top of the glass act as “electrodes” for the model.

Using the capacitor model, we were able to determine the Ground and Terminal domains for our model, set up a frequency domain based COMSOL Study, and implement a global COMSOL equation for measuring the admittance over a range of frequencies. The University of Southampton cellular model helped us translate the physics components of the capacitor model into the context of human skin.

1.5 Market Needs Analysis

As mentioned before, many skin phantoms look at addressing optical and electrochemical properties. However, there are challenges in adhesive biowearables such as wearable insulin pumps. When the electrical properties and adhesive of the device interact with moving and moisture changing conditions of the skin, issues with the longevity of the device and connection to what it is monitoring can be compromised. As a continuation of the previous two years working with Proteus Digital Health, the objective is to first create a skin phantom,

encompassing primarily the electrical and sweating properties of skin. Then, to optimize the mechanical properties. In the previous two years, research teams worked with Proteus' wearable device that was located on the abdomen. While this year, the team was no longer in connection with Proteus, the goal remained clear to create a skin phantom and computer simulation that could be used to test a wide variety of biowearable devices. Figure 1.5 depicts the various uses and needs of our target customers (bio-device companies and testing groups) in the biowearable device field.

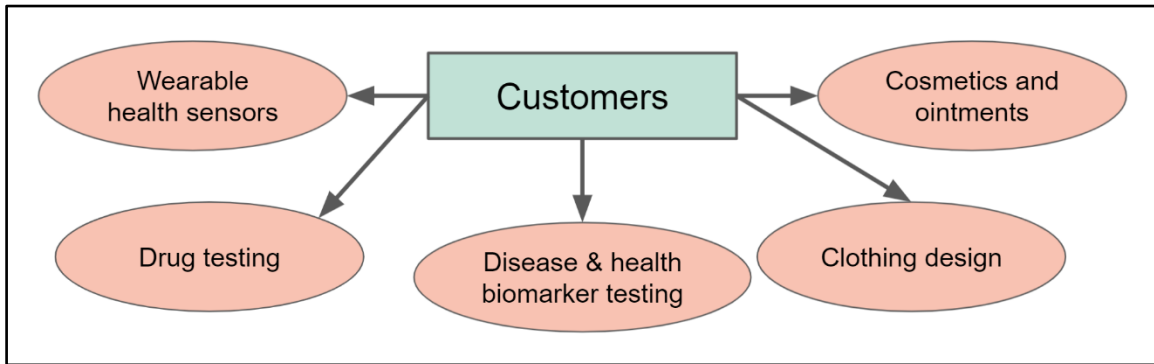


Figure 1.6: Target customer needs for biowearable companies.

Chapter 2: The Skin Phantom System

2.1 System Overview

As mentioned previously, our goal is to design a skin phantom using a gelatinous layer and silicone to mimic the impedance and perspiration behavior of the skin. An illustration of our system can be seen in Figure 2.1, which includes a physical model and computational model as the subsystems. For our physical model, we chose agar for the gelatinous layer that represents the dermis and silicone for the layer that represents the epidermis. For our computational simulations in COMSOL, we chose to simplify our model by only modeling the stratum corneum, the topmost layer of the epidermis.

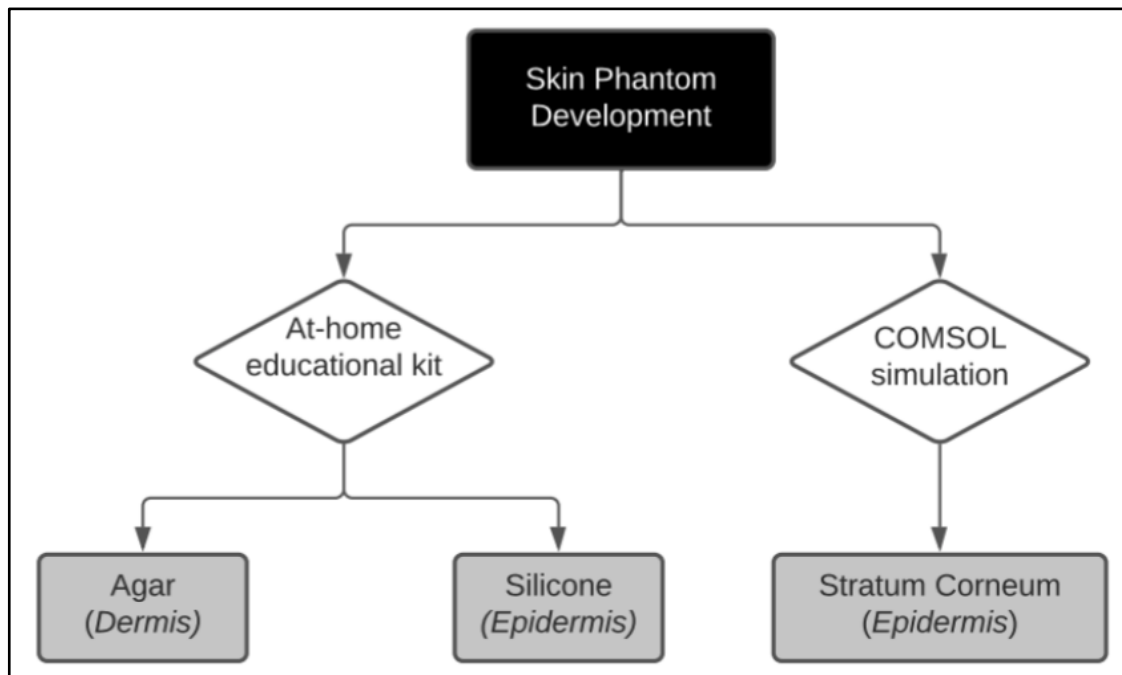


Figure 2.1: Systems level diagram of skin phantom testing.

2.2 Subsystem Goals

We will be separating our paper by the two subsystems: the Physical Model (also referred to as the educational kit) and the COMSOL Model Simulations.

2.2.1 The Physical Model Subsystem

As mentioned, our physical model is composed of agar and silicone layers. While it may not be optimal for a research setting, our project is an educational kit that aims to educate children and students on how different factors affect measurements that are taken on skin. These measurements include the addition of salt, which mimics the perspiration of skin, and pore size, which can affect the current traveling through the skin for biowearable devices. This will ensure that our phantom is customizable so that the students can problem-solve and decide which parameters are best for the desired behavior. Additional goals we have for our kit are to make it easy to manufacture, affordable, long-lasting, and sustainable. This subsystem will be elaborated upon in Chapter 3: The Physical Model.

2.2.2 COMSOL Electrical Data Simulation

The COMSOL model's objective is to obtain a basic understanding of the electrical properties of the skin. For our research purposes, the model needs to begin at a small scale so we can closely monitor how parameter changes impact the model's behaviors, specifically focusing on surface impedance over a range of frequencies. Starting small also helps cut down experiment processing times. The best way to determine how well the simulation is working is by comparing the simulation to real human skin. Therefore, the main goal of the COMSOL model is to create a functional computational model capable of simulating the basic electrical properties of human skin using real skin parameters. Eventually, the simulation model can be expanded to more realistic sizes with varying materials and material properties to test which simulates skin the most accurately. This subsystem will be further explored in Chapter 4: COMSOL Simulations of the Skin Phantom.

2.2 Integration of Subsystems

For the integration of both the physical model and COMSOL simulation, the merging of these two subsystems is used to create an educational kit. With the COMSOL model, the educational kit changes the focus to be more towards college-aged students. This is due to limitations that there may be at the high school level having access to the COMSOL program. The combination of the two can show how close the agar and silicone layers

represent the simulated skin. Eventually, even be able to change the material and material properties on COMSOL to try to find the best combination.

The other portion of integration of these two systems is by using the agar and silicone model to design the end goal of the COMSOL simulation. At this time, the model is in its simplest form with only one layer, the stratum corneum. However, human skin is multilayered, with each layer contributing multiple different properties, whether it be mechanical or electrical. Combining the agar-silicone physical model and the COMSOL simulation model is what will ultimately help bio-device companies the most in the future. By being able to test for specific properties by inputting the desired materials, a company can complete extensive testing before any money is spent on materials for the first iteration of their skin phantom with their device.

Chapter 3: The Physical Model

3.1 Overview of Subsystem

The physical model of our skin phantom utilizes biomimicry to imitate the physiological and electrical properties of the skin. We added salt to model the skin's conductivity and made the pores in our phantom representative of the pore size of skin. Overall, our materials were chosen to mimic the properties of the epidermis and dermis.

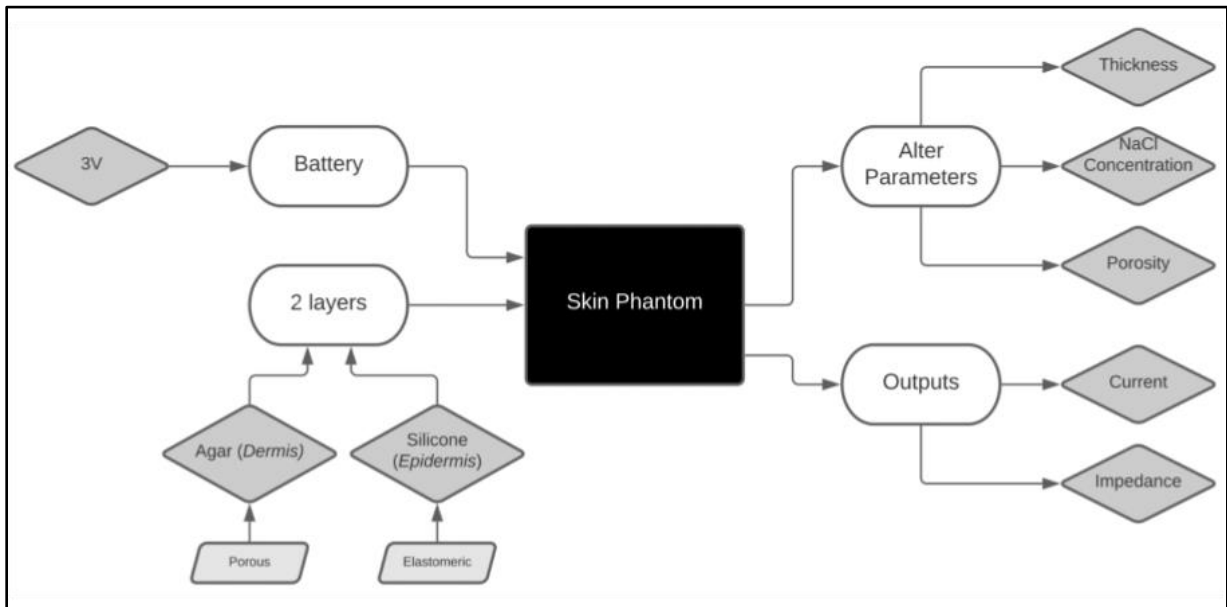


Figure 3.1: Systems level flowchart of inputs and outputs in physical model.

3.2 Material Choice

While the previous skin phantom team chose to use PDMS and carbon-black, our team improvised at home by using 4% agar for the dermis and porous silicone for the epidermis.

Agar is a hydrophilic polysaccharide extracted from seaweed. Dehydrated agar powder is first dissolved in boiling water and then cooled to form a gelatinous solid matrix. We chose this material for the dermis because, in addition to being biodegradable, it is a sustainable, raw material. It is easy to modify in terms of changing the thickness and adding salt for conductivity, and it can be made to have a similar density to skin [19]

For the epidermis, we used Ecoflex Super Soft Platinum Silicone to represent the viscoelasticity of skin due to its shore hardness of 00-50 [20]. It is also non-toxic, simple to assemble through mixing in a 1:1 ratio, and can remain stable for a long duration of time. This increases its ease-of-use outside of a lab for an application such as an educational kit.

However, to replicate the effect of perspiration on the conductivity of the skin, the silicone needs to be made porous. While more complex skin phantoms use laser-cutting or micromachining techniques, we were unable to access this equipment, and it would certainly not be available to the traditional student. By using sugar/salt leaching techniques and surgical tape, we were able to make our methods far more accessible because they do not require sophisticated laboratory equipment or hazardous solvents, which are typically required for etching [21], [22]. The caster sugar is about 200 microns, the size of an average sweat pore on the abdomen, making the model an accurate representation.

3.3 Fabrication

Our skin phantom consists of two layers, porous silicone and 4% agar with NaCl, to replicate the top two layers of skin, the epidermis and dermis, respectively (Fig. 3.2). Each layer is prepared separately and then stacked for the measurement of current.



Figure 3.2: Skin phantom assembly with porous silicone and 4% agar with NaCl.

3.3.1 Agar Layer

The agar layer, which models the dermis, was fabricated with the addition of salt for conductivity (Fig. 3.3). The inside of a square BIPEE Polystyrene petri dish was first wrapped in plastic wrap. Then, 2 g of dehydrated agar powder and NaCl was measured on filter paper and added to 50 mL of filtered water in a glass. This same ratio of 4% agar was

used for testing 75 mL and 100 mL of filtered water in additional experiments on the thickness of agar. The amount of NaCl varied so that the solution was 0%, 0.2%, and 1% NaCl. The mixture was microwaved in 30 seconds intervals until boiling and then immediately poured into the plastic-lined petri dish. The sides of the dish were tapped to remove bubbles. After sitting for 1 hour, the agar was solidified to the consistency of Jell-O.

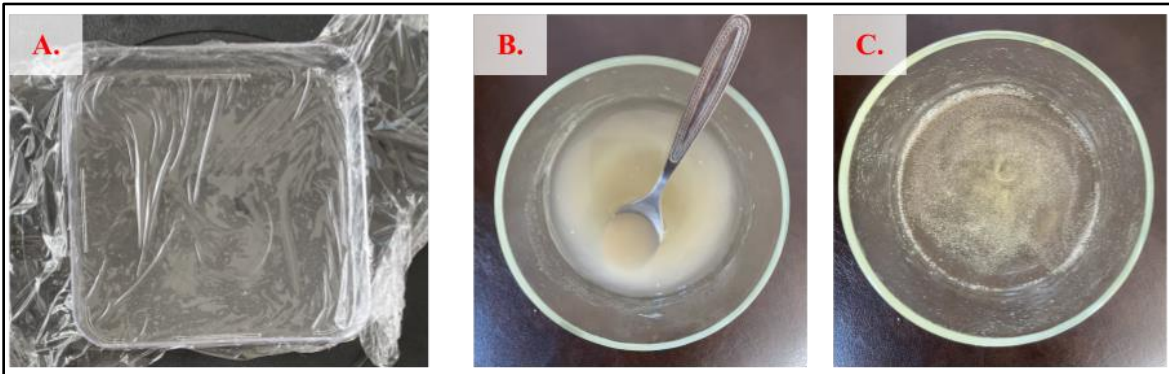


Figure 3.3: Making the agar gel. (A) BIPEE Polystyrene petri dish covered in plastic wrap. (B) Filtered water, dehydrated agar, and NaCl mixture (B) before and (C) after microwaving at which point bubbles should form.

3.3.2 Silicone Layer

The silicone layer replicates the epidermis and is therefore put on top of the agar. To formulate it, we prepared 15 mL of Ecoflex Super Soft Platinum Silicone. We added 5 mL of caster sugar and stirred for 5 minutes. The caster sugar was filtered through a 200 micron mesh bag to ensure it is accurate to the sweat pore size of the abdomen [23]. On our turn table was one part of the square petri dish (open-side down). We poured the silicone mixture on the surface of the dish, and spun the turn-table in a fast motion in order to “spin-coat” the layer. This allowed excess silicone to drip off of the edges (Figure 3.4). This was left to cure at room temperature for 12 hours or overnight. After this time, we were able to peel the silicone off of the petri dish, and it was ~5 mm in width.

To leach the silicone, we place it inside a thermos that was filled with boiling water. The thermos was sealed for 48 hours. After this time, we carefully removed the silicone, which

felt grainy to the touch due to the sugar that was leached out [24], [25]. The last step was to place the silicone on a paper towel and pat it until dry before placing it on top of the agar.

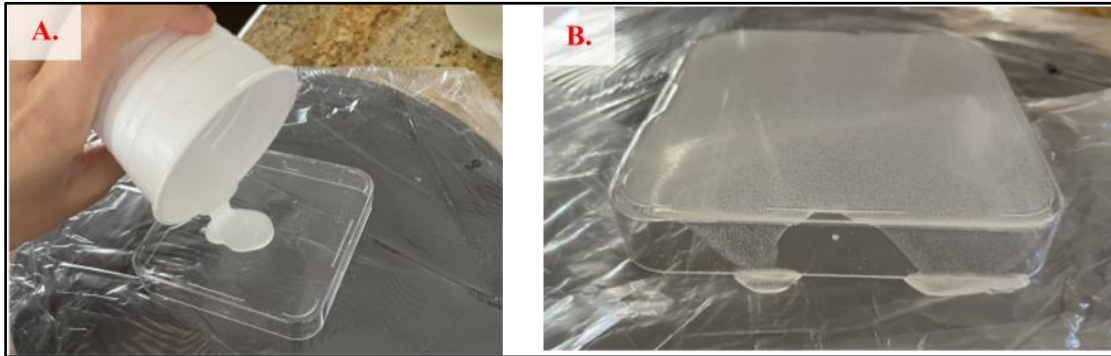


Figure 3.4: Creating the silicone molds. (A) Pour silicone mixture onto the petri dish, top-side down. (B) Spin turn-table rapidly for 5 minutes or until excess silicone has dripped off edges.

Since we did not receive a current with the 5 mL of sugar, we also experimented with combinations of sugar and salt, as well as replacing this silicone layer with microporous surgical tape (Fig. 3.5). The first involved mixing salt and sugar to the silicone in 1:1 ratios of 5 grams each before curing. In the next experiment, 5 grams of salt was added to the boiling water, in hopes that it would diffuse into the pores which the sugar leaches out of. In a similar vein, the third experiment involved soaking the already leached silicone in water with 5 grams of salt. Finally, in our last enhancement experiment, we poured water with 5 grams of salt onto the already leached silicone and let it sit overnight.

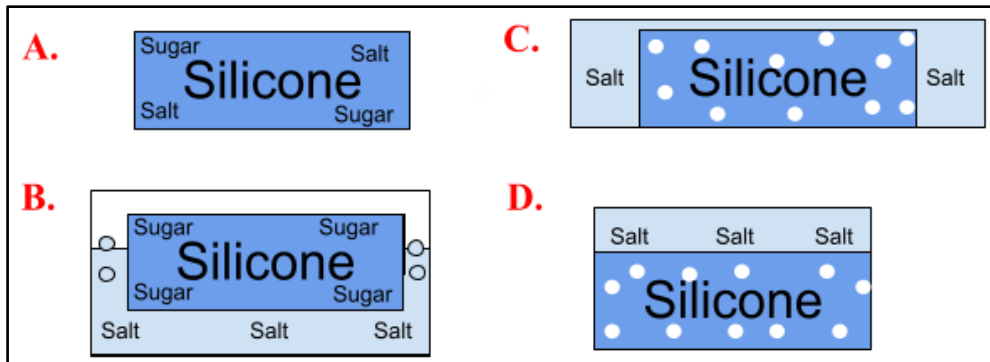


Figure 3.5: Enhancing porous silicone with salt. (A) Salt and sugar leaching. (B) Add salt to boiling water while sugar-leaching. (C) Soaking sugar-leached silicone in saltwater. (D) Pouring salt water on top of sugar-leached silicone.

For the final educational kit, the silicone layer may be replaced with Transpore Surgical Tape, a perforated plastic backed by transparent Polyethylene [26]. We chose this tape for its moderate stretch and microporosity. When tested with just one layer (Figure 3.6), we received a very high current, leading us to question whether the current was actually only coming from the agar. Therefore, we used a double-layer of the tape to ensure that the current was flowing only through the pores of the tape and not through the tape itself. The silicone layer was put atop 4% Agar of 1 cm width, and all future experiments utilized coplanar electrodes with electrode gel.

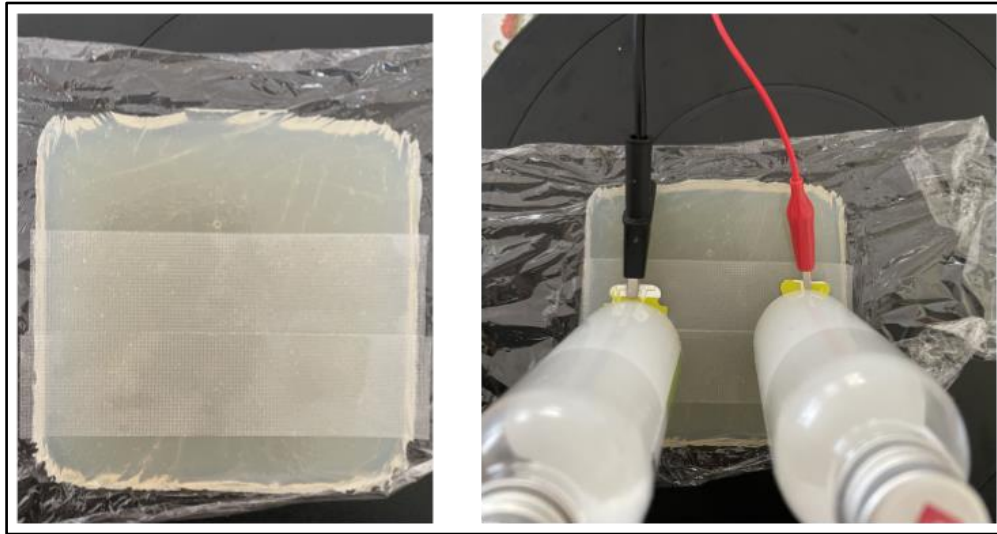


Figure 3.6: Simulating epidermis with Transpore Surgical Tape.

3.4 Electrical Data Collection

The voltage supply used in our experiments was provided by a 3V lithium coin battery. This was connected to one electrode, while the other electrode on our phantom was connected to ground (Fig. 3.7B). Hot glue was used to seal the battery with jumper wires (Fig. 3.7A), which were connected to alligator clips [27]. A heavyweight was placed on each electrode to maintain contact between the electrodes and the gel surface (Fig. 3.7C).

The initial experiments were run on only the agar layer to see the impact of salt concentration, thickness, and electrode placement on conductivity. Figure 3.8 below shows the electrode placements used, which were contraplanar (exist on different planes) and coplanar (exist on the same plane). The coplanar electrodes also had Spectra 360 Electrode Gel added to see if it would increase the conductivity.

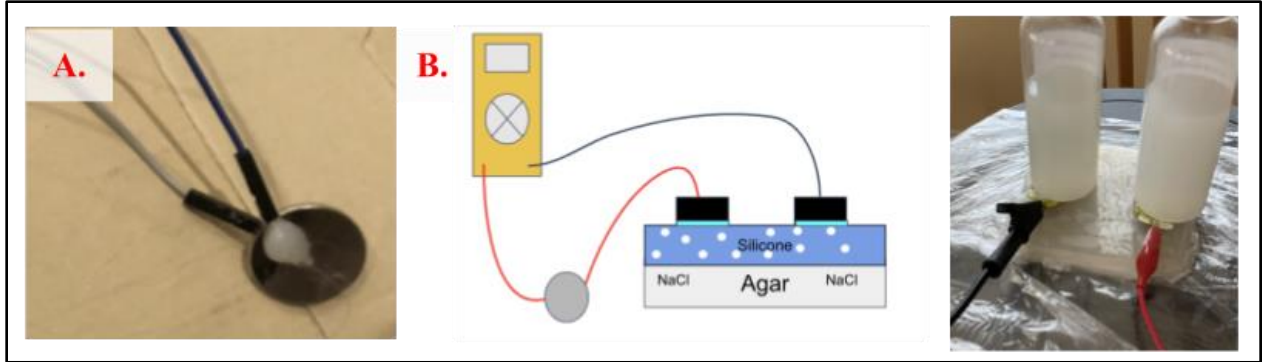


Figure 3.7: Setting up the educational kit circuit. (A) Hot glue used to attach wires to 3V coin battery. (B) (left) Final electrode setup with a digital multimeter (yellow) connected via alligator clip wires to the coin battery and electrodes on the silicone surface. (B) (right) Actual model setup for measuring agar resistance. Bottles act as heavyweights to maintain electrode-silicone contact.

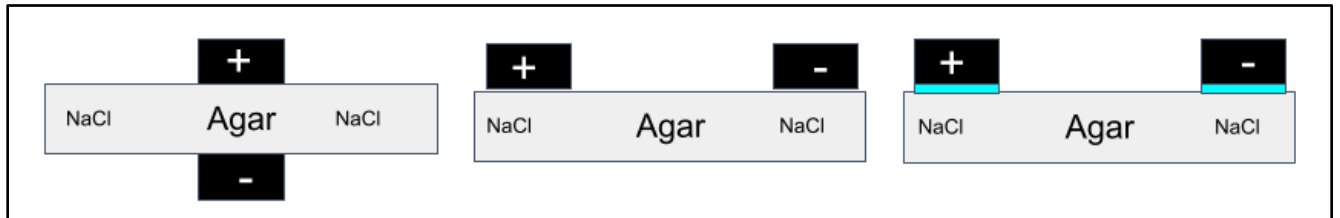


Figure 3.8: Electrode configuration for gel model. (A) Contraplanar. (B) Coplanar. (C) Coplanar with Spectra 360 Electrode Gel applied. Salt was added during the boiling process of the agar to create final concentrations of 0%, 0.2%, and 1%. The thickness of the agar was adjusted by simply making more of the agar solution. Adjusting the volume of water and dehydrated agar accordingly, we created agar thicknesses of 0.5 cm, 1.0 cm, and 1.5 cm.

Chapter 4: COMSOL Simulations of the Skin Phantom

4.1 Overview of Subsystem

This subsystem was completed using COMSOL Multiphysics® simulation software. Our COMSOL model aims to simulate the electrical and sweating characteristics of the stratum corneum of the epidermis' uppermost layer. This involves a single layer of the stratum corneum with sweat pores dispersed evenly across the model. In its simplest form, the model consists of the stratum corneum, skin pores, sweat pooling, and electrodes.

Initially, our COMSOL model was meant to serve as a temporary aid during our literature review while we waited for the campus labs to reopen. Still planning on continuing the previous skin phantom team's work with PDMS and carbon black, the original purpose of the COMSOL model was as an application of our research about the electrical and sweating properties of the skin and of the materials (like PDMS) which we would be using in our actual lab model. Due to continued campus closures, uncertain lab access, and a shift in our project's focus, the COMSOL simulations became our primary means of developing a skin phantom model for the hypothetical testing of biowearable devices.

In our simulations, we were planning on testing different materials and geometries, like conical vs. cylindrical pore shapes, as well as various factors from our physical model experiments. Seeing that none of us had proper training or experience working with COMSOL prior to the start of this project and we did not know it would become an integral feature of our project until late fall 2020, we had a steep learning curve to overcome. We were mostly successful, but our model designs and simulation tests were still limited as a result of this learning curve, so we were unable to test everything we initially wanted to.

For the purpose of our project, the surface impedance was measured over a range of frequencies in the presence of various sweating environments, primarily that of surface sweat pooling and electrode spacing.

4.2 Software

COMSOL Multiphysics 5.5 Academic Class Kit License was used to run all simulations in this project. The computer requirements to run COMSOL 5.5 are at least 4 GB of memory, Adobe Acrobat Reader, and Intel or AMD CPU 64-bit processor [28]. To convert the COMSOL data of admittance vs. frequency into impedance vs. frequency plots for each dataset, MATLAB R2020a program was used. This process is explained in further detail in Section 4.4: MATLAB. The computer requirements to run MATLAB are at least 4 GB of memory, a disk with 3GB of HDD space, and an Intel or AMD CPU 86-64 processor.

COMSOL Multiphysics software is typically used for its multiphysics simulation capabilities and finite element analysis and solver. The software provides users with conventional physics-based interfaces that are paired with systems of partial differential equations to create an integrated development environment with a unified workflow for applications of electrical, mechanical, wave-based (including fluidic and acoustic), and chemical features.

4.3 Parameters

The parameters features in COMSOL are a useful tool to allow for easy changes to the model's properties and characteristics to test different variables. Our model utilizes global parameters for our notable variables to streamline the experimentation process by keeping all the desired independent and dependent variables in one location rather than dispersed under the different component features like geometry, materials, and physics. In Global Parameters, abbreviations of the variables and geometry names were made with their respective values. These global parameters not only improve our design testing efficiency, but also the model's use in future testing applications. With the global parameters, the model can be easily changed depending on the specifications of the skin phantom to be replicated and/or the biowearable device to be tested. The user can simply access and edit the desired values of their materials and run the simulation without requiring any drastic changes to the model's skeletal structure. The parameters used in our standard model are shown in Table 4.3.

4.3.1 Geometry and Material

The geometry and material parameters define the size, shape, material, and associated physics-related properties of the model. In Table 4.3, the geometry parameters can be seen with the size and material in the same row. In this simulation, only two materials were used, air and polydimethylsiloxane (PDMS). While realistically, human skin is composed of much more, the idea is to use a material that has similar characteristics but can be easily changed when needed. While we used the PDMS and air materials within COMSOL, the property variables critical to the electric current physics module (relative permittivity and conductivity) are overwritten with actual values from the stratum corneum, sweat, and electrodes. For our simulation studies, the electrical conductivity and relative permittivity of each material domain are the most important material properties for the physics calculations, so these are the only values we replaced with proper skin-sourced values. Since COMSOL understands the function and usage of each property variable in its physics modules, changing the value of these variables doesn't cause issues with the simulation or calculations.

Table 4.3: Parameter names and values in COMSOL. The parameter names and values that were set for the baseline model. Depending on what was being tested, certain variables such as sweat pooling had a range of values. This table also depicts the material of the region.

| Geometry | COMSOL Abbreviation | Size (um) | Base Material | Notes |
|------------------------|---------------------|--------------------|---------------|----------|
| Pore Height | <i>PoreHeight</i> | 1000 | PDMS | |
| Pore Radius | <i>PoreRadius</i> | 100 | PDMS | |
| Distance Between Pores | <i>DistPore</i> | 1000 | PDMS | |
| Epidermis Radius | <i>PDMSradius</i> | 2500 | PDMS | |
| Epidermis Height | <i>PoreHeight</i> | 1000 | PDMS | |
| Electrode Height | <i>ElecHeight</i> | 500 | Air | |
| Electrode Width | <i>ElecSize</i> | 1000 | Air | |
| Sweat Pooling Height | <i>PoolHeight</i> | 0-500 | PDMS | Variable |
| Sweat Pooling Radius | <i>PoolRadius</i> | 100, 150, 200, 250 | PDMS | Variable |

4.3.2 Physics

The key electrical properties of our model focus around resistance, permittivity, conductivity, and impedance. In its simplest terms, the model is composed of a resistor and capacitor in series, as illustrated in our diagram (Fig. 4.1). However, COMSOL is able to carry out the complexity of models in a mathematical format for us.

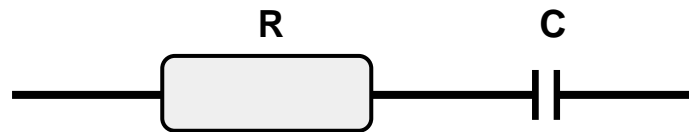


Figure 4.1: Resistor and capacitor in series.

Resistance can be characterized by rho (ρ) multiplied by length (L) divided by the area of a bounded region (A) (Fig. 4.2). If two conducting plates are separated by a non-conducting material, it forms a capacitor whose capacitance value is determined by the plates' sizes, distance apart, and the non-conducting material's electrical properties (Fig. 4.3) [29]. The non-conducting material is called the dielectric. Capacitance is characterized by the permittivity of free space (ϵ_0 , electric constant) multiplied by relative permittivity (ϵ_r , dielectric constant) and the surface area of a plate (A), all divided by the distance (d) between the two plates (Fig. 4.3) [29].

$$R = \frac{\rho L}{A}$$

Figure 4.2: Resistance equation.

$$C = \frac{\epsilon_0 \epsilon_r A}{d}$$

Figure 4.3: Capacitance equation [29].

Permittivity of free space is a physical constant while relative permittivity depends on the material [29]. In our model, relative permittivity is used. Permittivity is a constant property of a material, while conductivity is a dynamic property of a material. This means that for a given material, its permittivity will stay constant (unchanging) but its electrical conductivity can change or vary. Electrical conductivity is proportional to the admittance, which is a measure of how easily a circuit allows a current to flow through it. Impedance is the opposition to the flow of electric current through a material, making impedance the opposite of electrical conductivity (Fig. 4.4). In short, as the conductivity and permittivity increases, the impedance will decrease due to reduction in resistivity.

Capacitors often behave non-ideally, acting like a constant phase element (CPE) [29]. This holds true in the case of real cells, as the “double layer capacitor” they form often behaves more like a CPE than a true capacitor. For CPE, the α exponent is less than one rather than equal to one as is the case for true capacitors [29]. Although various theories have been proposed in an effort to explain the non-ideal behavior of this real cell double layer -- surface texture, non-uniform distribution of current, inconsistent or “leaky” capacitor, etc. -- but until confirmed, it is best practice to just treat α as an empirical constant [29].

$$Z_{CPE} = \frac{1}{(j\omega)^\alpha Y_0}$$

Figure 4.4: Impedance of CPE capacitor equation. Non-ideal capacitor, constant phase element (CPE). $Y_0=C$ =capacitance. α =empirical exponent, w =radial frequency. [29]

COMSOL is unable to directly produce impedance data but we can get impedance values by having COMSOL measure admittance and using the mathematical relationships shown here. Since electrical conductivity is proportional to the admittance and impedance is the opposite of conductivity, this means the impedance is the inverse of admittance (Fig. 4.5).

$$Y = \frac{1}{Z}$$

Figure 4.5: Relationship between impedance (Z) and admittance (Y).

4.3.3 Electric Currents Module

The priority physics used in our COMSOL was Electric Currents, added from the “Add Physics” tab, to retrieve the admittance vs. frequency plot points to later change into impedance vs. frequency in MATLAB. Within Electric Currents, the current conservation, electric insulation, initial values, terminal, and ground were added. Current conservation is domain-based so all domains of the model are selected and overridden later if needed. Next is electric insulation, which is boundary-based and has all the model’s boundaries selected. Then, the initial values are domain-based, selected by all, with an electric potential (V) value of 0 V. The terminal is domain-based and is selected by the cathode, while the ground is boundary-based and selected by the bottom face of the anode. The next part is followed by adding necessary conductivity and relative permittivity values under the material’s properties. See Appendix D.1: Current Conservation Equation for further insight into the systems of partial derivative equations used as a part of the frequency domain study in our model. Table 4.4 shows the values of conductivity and relative permittivity respectively to each feature. Other values were tested for both conductivity and relative permittivity, which are shown below each feature respectively, and will be talked about in more detail in results.

Table 4.4: Conductivity and relative permittivity values for model features. These values were adjusted to see the potential impact each had on the overall impedance. When testing these properties, only one was changed at a time.

| Feature | Conductivity (S/m) | Relative Permittivity |
|------------------------------|--------------------|-----------------------|
| Epidermis | 1×10^{-6} | 2.5 |
| | 1×10^{-7} | 72.9 |
| | 2×10^{-5} | 86 |
| Pores and Sweat Pooling [30] | 1×10^{-4} | 2 |
| | 1×10^{-2} | 55.5 |
| | 1 | 80.2 |
| Electrodes | 0 | 1 |

4.3.4 Frequency Domain Study

Skin impedance varies with respect to the frequency of the applied signal, so we had to determine an adequate frequency range [7]. Last year's skin phantom team worked with a bio-device company called Proteus Digital Health who wanted a skin phantom on which they could test their biowearable device. Proteus' device operates in the 10-20 kHz range; however, we tested our model over a frequency range 2-20 kHz to allow for more application opportunities and to test the limits of our model [2].

Our model uses a frequency domain stepwise study to “step” through a range of frequencies and measure the result of the electric currents module. The range steps in increments of 1 kHz from 2 kHz to 20 kHz. For more precise data and smoother impedance vs. frequency plot lines, the frequency step can be decreased to 500 Hz, or 0.5 kHz, without increasing the processing time of the model too drastically.

4.3.5 Evaluation Expressions for Admittance

From the COMSOL library Capacitor model we obtained a library expression we can use within COMSOL to measure the admittance of the model. The expression “ec.Y11” with unit S uses the dataset produced from the frequency domain study of the electrical properties of the model. This expression is entered into the Global Evaluation add-in under the Derived Values tab in Results and used to produce 1-D Plots for the admittance results. COMSOL produces both real and imaginary parts using “real(ec.Y11)” and “imag(ec.Y11),” respectively, in the global evaluations add-in for each 1-D Plot. These expressions call to an internal mathematical library to produce the real and imaginary admittance matrices. See Appendix D.2: Complex Impedance for RC Circuit for diagrams and equations explaining the relationships between resistors and capacitors with imaginary and real data [31]. For our project's admittance data, we want the imaginary data; thus, the imaginary part of the admittance matrix is the data later exported to MATLAB.

4.4 Models

4.4.1 Preliminary Model

Based on the Capacitor model found in literature review, our preliminary model consisted of small and large air cylinders surrounding a porous epidermis layer (Figure 4.6). As color-coded in Fig. 4.6, this initial model consisted of a middle PDMS layer (grey) with several cylindrical tubes cut out and filled with liquid to represent sweat pores in the epidermis (lime green). The PDMS layer is sandwiched between two cylindrical-disc layers of air and two thin cylindrical tubes (light pink). These air cylinders act as electrodes to measure the admittance of the surface of our model.

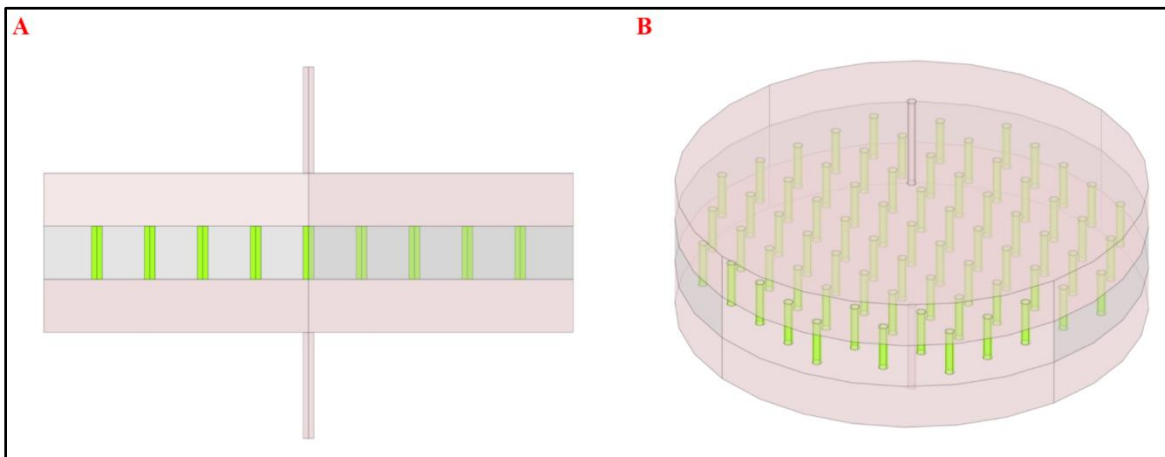


Figure 4.6: Preliminary COMSOL epidermis model. (A) Side view. (B) Isometric view.

Through experimentation we found these many air cylinders to have minimal impact on our models' experimental values, so our model simplified to include just two square electrodes on the epidermis surface to perform the measurements necessary in our simulation.

4.4.2 Final Model

For the most part, our final model builds off of the preliminary model with the addition of square electrodes and pore sweat pooling on the epidermis surface. Fig. 4.7 and 4.8 present various views of our final model. The model still consists of an epidermis layer, shown in grey, with sweat-filled cylindrical pores, shown in lime green. New to this version are pools

of sweat on the model surface above each pore, shown in dark blue. Our model lacks fluid mechanics, so for our simulations we used sweat pools of different heights and radii to represent different volumes of surface sweat pooling and consequently, varying perspiration rates. In purple and light blue are the anode and cathode electrodes, respectively, which are positioned over the top of pores. Fig. 4.8A shows our final model labeled as described.

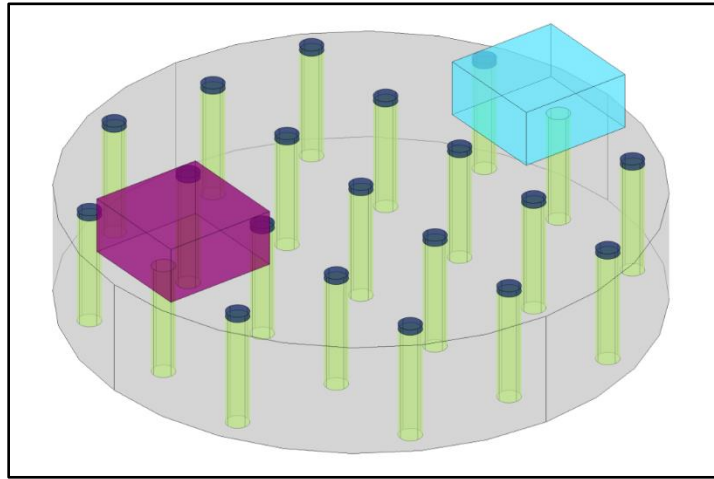


Figure 4.7: Isometric view of final COMSOL epidermis model.

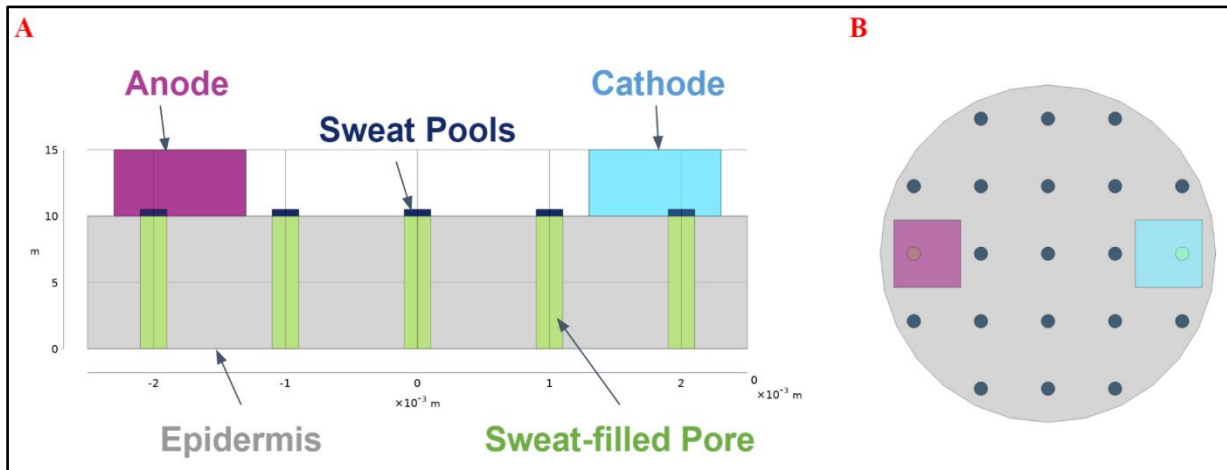


Figure 4.8: Further views of the final epidermis model. (A) Side view with labels. (B) Top-down view. Note green inner-pore sweat visible through the electrodes, representing the lack of sweat pooling beneath the electrodes.

To improve run times, our model was reduced to a 5000 μm , or 0.5 cm, diameter while keeping the pore spacing and radius the same to remain accurate to what a to-scale model

would have. With our scaled-down model, simulations finish in minutes rather than a half hour or longer. This is helpful for testing the performance of our model; however, this would need to be scaled up to appropriate size before being used to test biowearables. Our global parameters allow for such adjustments to match the model to that of the desired skin area.

4.5 MATLAB Code

Upon running our simulation, COMSOL produces various color plots and line graphs of variables like electric potential and frequency. While these are useful visuals for ensuring our experimental set up was working properly, we chose to export the numerical data to MATLAB for more in-depth analysis capabilities. In addition, the COMSOL study only outputs admittance dataset (see Section 4.3.4) so we utilized MATLAB to convert this data into impedance values and plot impedance vs. frequency (Fig. 4.9).

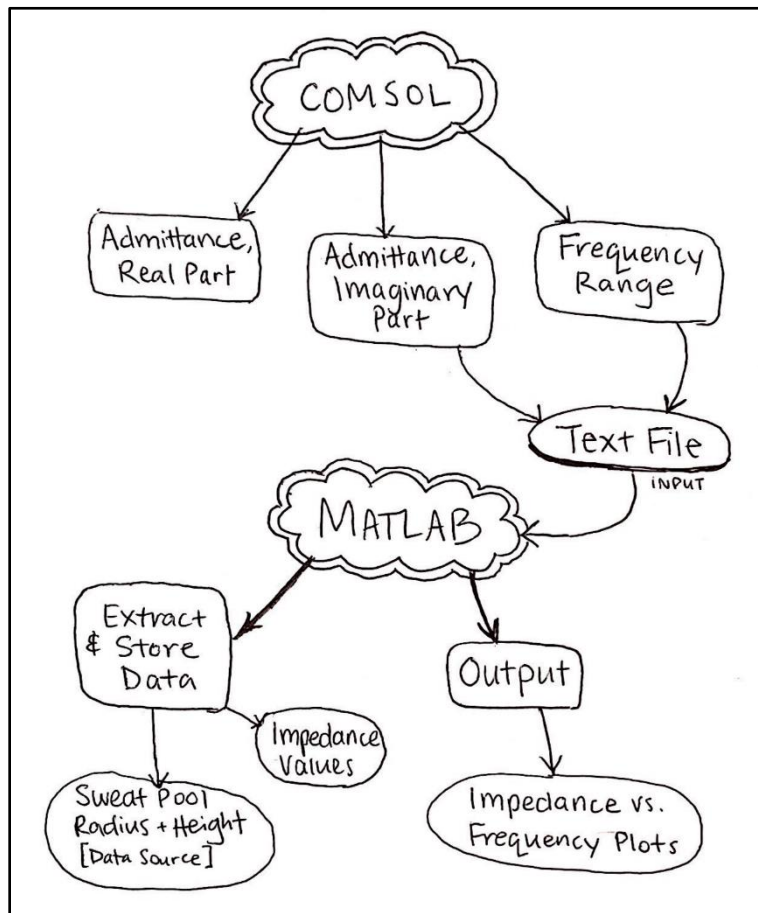


Figure 4.9: Systems level flowchart of COMSOL-to-MATLAB pipeline.

4.5.1 Initial Data Preparation

Initially, we would just copy the raw admittance vs. frequency data individually from each COMSOL run and paste it directly into a simple MATLAB script to calculate the impedance and plot it vs. frequency. This proved to be very tedious and time-consuming as the data had to be seriously reformatted each time it was pasted into the script. To aid this data transfer process, we implemented a “Export Plot Data” component to our simulation using the Exports tab of the Results section in COMSOL. This new feature allows us to export a desired dataset in the form of a text (.txt) file with a “spreadsheet” format and header lines noting the COMSOL model file used to produce the data, as well as the export time and date. See Appendix E.1: Example Text File Export from COMSOL for an idea of what one of these text files looks like. We chose to name our text files using a notation that both aids in separation of datasets during MATLAB processing and visual communication to the user what the file involves. Each text file is given a specific name that indicates which data set it belongs to and variables are changed in the MATLAB program to match those files accordingly. For example, data produced from a model with sweat pools of radius 100 μm and height 50 μm with no other changes made (such as electrical conductivity or relative permittivity or electrode distance) would be labeled “r100h50_orig.txt” upon export.

4.5.2 Program Function

To streamline our analysis process, we developed MATLAB programs to extract this data and plot multiple sets of text files at one time. The MATLAB program utilizes local functions and nested for loops to further improve the program’s efficiency. The drafted pseudocode for the program can be found in Appendix E.2. As seen in Fig. 4.9, the program is structured to receive user-input for the names of the text files exported from COMSOL that contain admittance vs. frequency data. The user-input can be either the full file name or as simple as listing the sweat pool radii and heights, and the abbreviation for the variable tested. For example, while testing electrical conductivity the variable suffixes used for the text files were “_ec0,” “_ec1”, and “_ec2” to represent which data were from the model with the original conductivity value and which were from the higher or lower conductivity values being tested.

The general progression of each program from this point is to: (a) find and open the specified text files (if no such file was found, the program stops and displays an error message), (b) scan the file (skipping the header lines) for data, (c) store extracted data (admittance and frequency values) in their respective variable, (d) calculate the impedance using the admittance, and (e) plot the impedance vs. frequency.

All of these steps (a-e) are completed using a series of local functions (Appendix E.4). This was done because these processes are ones that need to be run multiple times for different variable inputs, so rather than repeat similar blocks of code for each text file, we can keep the code clean and efficient by calling a local function instead. After this, the program continues to loop through whatever variable it is constrained by, ultimately outputting one or several figures with multi-line plots. Combining the local functions with nested for loops allows users to produce multiple figure plots with multiple lines on each plot in a single program run -- something that otherwise would have to be accomplished through really long code (lack of local functions) and/or in separate program runs in which the variables must be adjusted after each run (lack of nested for loops).

Appendices E.3 and E.4 provide an example of what our several MATLAB programs look like in terms of the main script and local functions' definitions. All of the code in A-E.3 and A-E.4 are extensively commented for clarity and ease of use.

Chapter 5: Results

5.1 Educational Kit

5.1.1 Agar Layer

To optimize our agar layer for conductivity, we took measurements with different placements of our electrode, as illustrated in Figure 3.5. We took 9 measurements for each test at varying thicknesses/heights of the layer (0.5 cm, 1 cm, 1.5 cm) and salt concentrations with the agar (0 %, 0.2%, 1 %). The results of the current and resistance measurements can be seen in Figure 5.1 and Figure 5.2, respectively. The leftmost plots represent a contraplanar electrode, while the center shows a coplanar electrode setup, and the rightmost plots show coplanar electrodes with electrode gel applied to enhance measurements.

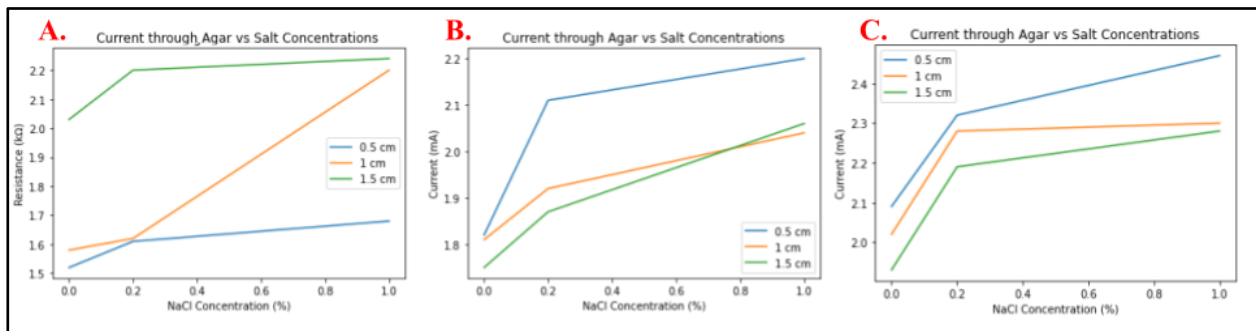


Figure 5.1: Resistance vs. NaCl concentration in 4% Agar of varying thicknesses (0.5, 1, 1.5 cm). Electrode placements: (A) Contraplanar, (B) Coplanar, (C) Coplanar with electrode gel.

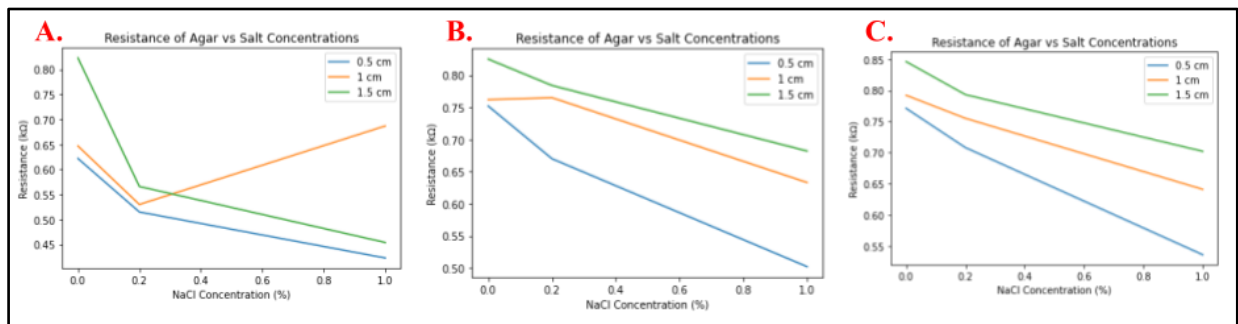


Figure 5.2: Current vs. NaCl concentration in 4% Agar of varying thicknesses (0.5, 1, 1.5 cm). Electrode placements: (A) Contraplanar, (B) Coplanar, (C) Coplanar with electrode gel.

Overall, there was a trend that as NaCl concentration increased, there was an increase in conductivity and therefore a decrease in resistance. Due to Kirchoff's law (voltage equals current times resistance, $V=IR$), a decrease in the resistance meant an increase in current because more electrons were able to flow through the agar. Additionally, there was a higher current as the thickness of the agar increased, because there was more surface area through which the current can flow.

For our subsequent experiments with silicone, we chose to test with contraplanar electrodes with electrode gel. This was because the electrode gel increased the amount of current able to flow. The silicone was placed on top of 1 cm thick agar with 1% NaCl agar because this thickness showed the most linear relationships with NaCl concentration. Additionally, 1% NaCl was small enough to avoid saturation but large enough to receive reliable results.

5.1.2 Silicone Layer

To make sure the current flowing through the agar was also flowing up through the silicone, the silicone layer needed to be made porous through the processes described in Section 3.3.2. However, no current passed through with just sugar grains, so we experimented with a mixture of salt and sugar, as well as with microporous Transpore Surgical Tape.

The silicone shown in Figure 5.3 shows that even a small amount (1 gram) of sugar created micropores; however, the pores were not abundant enough to become interconnected. The pores were scattered throughout the silicone, so no current would be able to pass through pores on either end of the layer. As shown in Table 5.1, there was still no current passing through the silicone when we increased the sugar to 5 grams. This led us to experiment with salt, which we found needed to be combined with the sugar in order to receive a current. This may be because while the sugar provides essential pores for the current to flow, the salt provides conductivity, just as it did with the agar layer.



Figure 5.3: Porous silicone gel made with 1 g sugar in 15 mL silicone.

From our salt experiments, illustrated in Figure 3.5, the “sugar and salt leaching” and “saltwater pour” proved most fruitful in terms of current flow. These results suggest that salt cannot easily diffuse into the agar through osmosis but needs to be directly added into the silicon mixture or into a solution that makes direct contact with the electrodes. The Transpore Surgical Tape also resulted in high amounts of current flow, and we saw a decrease with two layers, as expected. This is most likely due to the current with only one layer of surgical tape coming from the conductive agar, rather than through the pores of the silicone. We would urge future teams to test these layers individually (without agar) to ensure that the silicone is in fact porous and that current can flow through it.

Table 5.1: Current flow for silicone layers on top of 4% Agar with 1% NaCl.

| Epidermis Layer Tested | Current |
|--|----------------|
| 1 g sugar | 0 |
| 5 g sugar | 0 |
| 5 g salt | 0 |
| 5 g sugar + 5 g salt | 11.7 uA |
| 5 g salt + 5 g sugar + saltwater pour | 1.453 mA |
| 1 layer of microporous tape | 1.50 mA |
| 2 layers of microporous tape | 0.47 mA |
| 2 layers microporous tape + saltwater pour | 1.314 mA |

5.2 COMSOL Simulation

In our COMSOL simulations, we achieved a small-scale simulation of the stratum corneum, the most top layer of the epidermis. We tested our model with simulated electrodes to look at how pores, sweat pooling height and diameter, and electrode distance impact the impedance over a range of frequencies. With the current simulation, the materials reflect that of the stratum corneum and NaCl sweat properties.

5.2.1 Sweat Pooling

Many difficulties in biowearables have to do with the amount a person begins sweating. Multiple difficulties such as adhesion and electrical readings may vary due to the amount a person is sweating [32]. The first goal for the COMSOL simulation was to see how much variability occurred depending on the amount of sweat pooling. For the simulation, we added another array of cylinders with PDMS material. The PDMS material is a placeholder due to the priority needed being the conductivity and relative permittivity of the material. Due to those values being imputed manually by the user, the material itself is not critical to the simulation.

The cylindrical sweat pool objects were placed on the top of each pore, respectively. Thus, these sweat pools exist on the surface of the epidermis and are flush to the plane of each pore's opening. An important note is that we omitted any sweat pooling cylinders under the electrodes due to an assumption the electrode is pressed tightly against the skin, thus preventing the pooling of sweat on the skin's surface. Although there is no sweat pooling under the electrodes in our model, the electrodes are still in contact with the surface of the sweat inside the pore it covers. A visual representation of this can be seen in Figure 5.4.

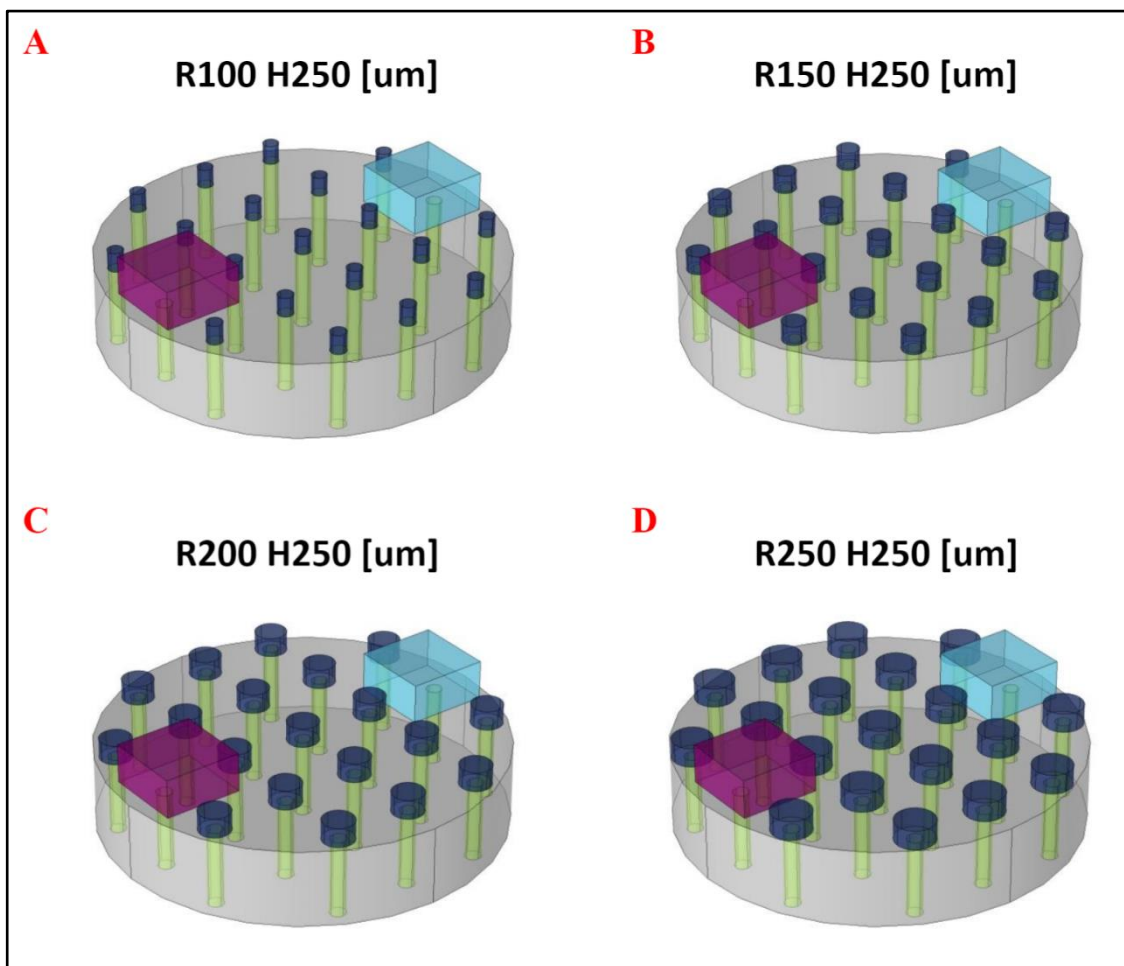


Figure 5.4: COMSOL diagrams in isometric view. All models shown here have 250 μm height sweat pools. Note the lack of sweat pooling underneath each electrode. (A) Sweat pools with radii of 100 μm , the same radius as the sweat pores, (B) 150 μm , (C) 200 μm , and (D) 250 μm .

With the sweat pooling cylinders in place, we tested various heights and radii of this surface sweat pooling to see if there was a trend in the impedance measurements of the skin surface over a frequency range. We tested radii in 50 μm increments ranging from 100 μm to 250 μm , essentially a saturated phantom. Next, the height of the sweat pooling was varied for each radius, ranging from 5 μm to 500 μm . Each variable combination is listed in Table 5.2.

Table 5.2 Correlating height and radius combinations tested for sweat pooling.

| Height (μm) | Radius (μm) |
|--|--|
| 5 | 100 |
| 5 | 150 |
| 5 | 200 |
| 5 | 250 |
| 500 | 100 |
| 500 | 150 |
| 500 | 200 |
| 500 | 250 |

After taking measurements for each variation, we compared the radii depending on the height. For these experiments, we varied only the radius of the sweat pools for a set height (5 μm and 500 μm). Impedance graphs for the two different heights of sweat pooling can be seen in Figure 5.5. In these experiments, the sweat pooling models were also compared to a control. For our control, we chose to use air because if the sweat pores are filled with air it equates to if there was no sweat present. This comparison also justifies the conductivity and relative permittivity of sweat resulting in a lower impedance.

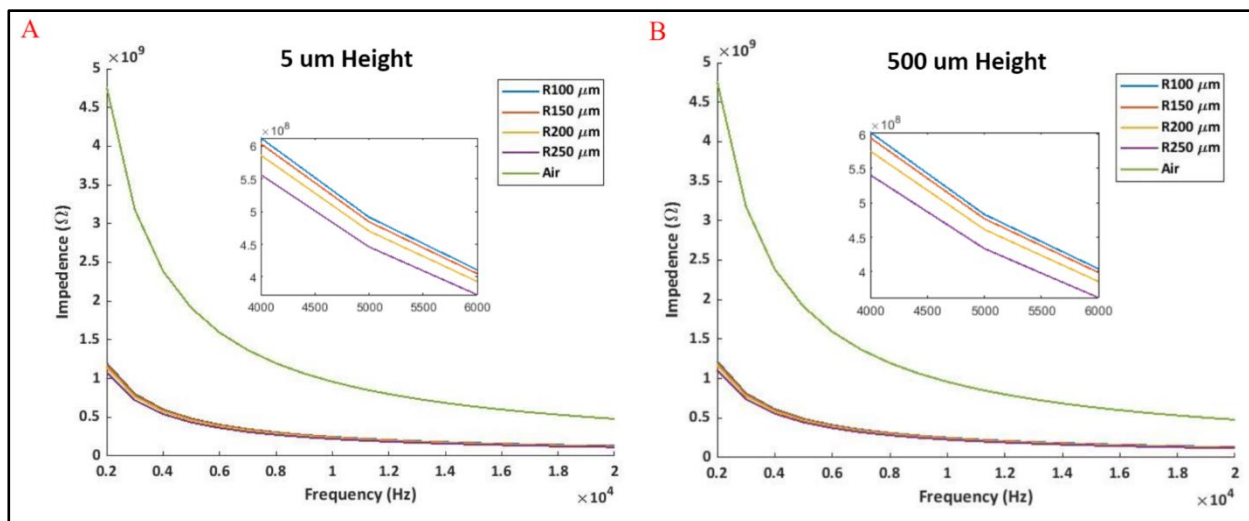


Figure 5.5: Impedance vs. frequency graphs for varying surface sweat pooling radii. Radii range 100, 150, 200, 250 μm with sweat pools height (A) 5 μm and (B) 500 μm . For the air material, there is no surface sweat pooling or sweat within the pores.

In Figure 5.5, the plots demonstrate that as the sweat pooling radius increases there is a greater decrease in impedance. The difference between 100 μm to 150 μm radii is slight but impedance begins to decrease at 200 μm and much more at 250 μm radius. This trend is the same for both heights, with minimal difference between the two heights' datasets. From 5 μm to 500 μm height sweat pools, the impedance does decrease slightly, evident by the 0.1 $\text{M}\Omega$ impedance drop of the 250 μm radius sweat pools. However, it can be concluded that the area against the skin has a greater effect on the impedance than the height of the sweat pooling.

5.2.2 Electrode Distance

Knowing the distance between anode and cathode alters the measurements our model detects, we tested different electrode spacings. For our small-scale simulation, three distances were chosen to see how the impedance changed based on the electrode distance. For the other simulations, the electrode distance was at the maximum distance of 2.6 mm. This distance was labeled as our “far” electrode distance. The “medium” distance was set to 1.26 mm from each side of the electrode and the “close” distance was set to 0.22 mm. The “close” distance is approximately the diameter of one pore, 200 μm . A visual for the electrode distances can be seen in Figure 5.6.

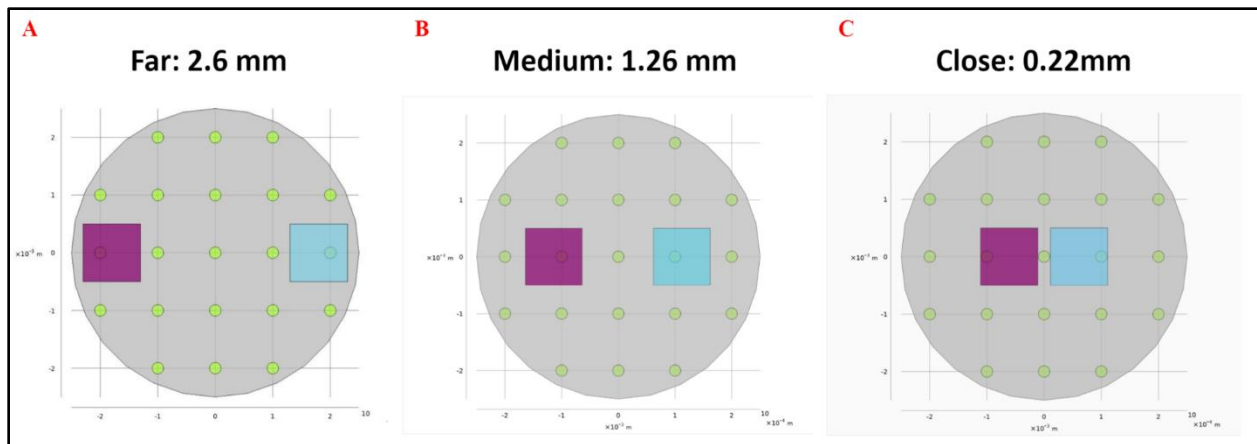


Figure 5.6: COMSOL top-down view of electrode distances. Distance is measured from the inner edge of each electrode to the right side of the purple electrode and the left side of the blue electrode. Electrode distances tested were (A) 2.6 mm, (B) 1.26 mm, and (C) 0.22 mm.

We expected that as the electrodes move closer together, the impedance should decrease as a result of there being less distance for current to flow through. The impedance vs. frequency graphs produced from these models are in Figure 5.7.

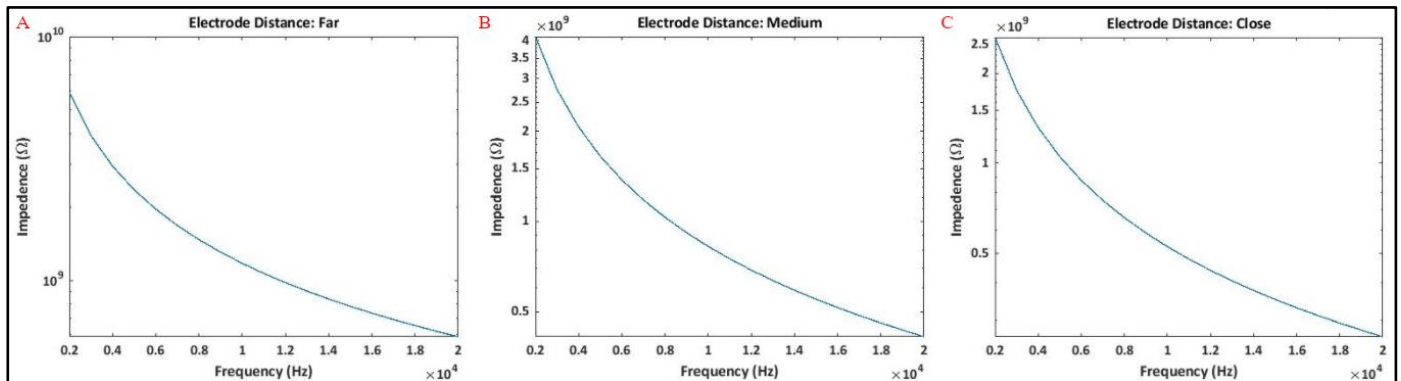


Figure 5.7: Impedance vs. frequency for varying electrode distances. (A) Farthest electrode distance at 2.6 mm. (B) Medium distance at 1.26 mm. (C) Closest distance at 0.22 mm.

The far electrode distance has the highest impedance compared to the medium and close electrodes, thus, confirming our expectation. The change is most evident between the medium and close electrodes as the impedance ranges shift from 4 to 2.5 Ohms in the same

magnitude. This experiment clarified that the simulation will have different values depending on electrode size and distance relative to the skin phantom size. This is important to know for when it comes time to scale up the model, as the ratio between electrode size and spacing may need to be maintained.

5.2.3 Conductivity and Relative Permittivity

The last thing tested was varying the conductivity and relative permittivity values of the stratum corneum and sweat. For a list of values, please refer back to Table 4.4. The standard values were observed from “A Cellular Model of the Electrical Properties of Skin on a Cellular Level” [17]. The stratum corneum has a conductivity of 1×10^{-6} S/m and a relative permittivity of 2.5. The following values for conductivity and relative permittivity vary from different conditions of the skin such as multiple layers of the stratum corneum [17]. For the sweat parameters, the standard values are 1×10^{-4} S/m for conductivity and 2 for relative permittivity. The conductivity values were chosen knowing sweat conductivity changes greatly depending on the person and diet due to the resulting variations in sweat compositions. The relative permittivity values for sweat were decided based on temperature changes of sweat affecting its value [30]. Testing the conductivity and relative permittivity for each stratum corneum and sweat dataset was done individually. For example, when testing for stratum corneum conductivity at 2×10^{-5} S/m, the relative permittivity stays at 2.5 and the sweat values remain constant.

First, we looked into testing our model using values for real sweat conductivity and relative permittivity (Fig. 5.8). The sweat relative permittivity had little to no change as the relative permittivity increased significantly. This data seems to say the permittivity is not having as great an effect on the impedance as was hypothesized. The relative permittivity of the stratum corneum, or epidermis, may explain why later on. For the sweat conductivity, going from 1×10^{-4} S/m to 1×10^{-2} S/m, the change in impedance makes sense. As the conductivity is increasing, the impedance is decreasing due to there being less resistance for the current to flow through. However, once the conductivity is increased to 1 S/m, the graph itself is not characteristic of an impedance versus frequency graph. This shows there is a limit

in the model. That limit is likely to be the size of the COMSOL model since the model is working on such a small scale.

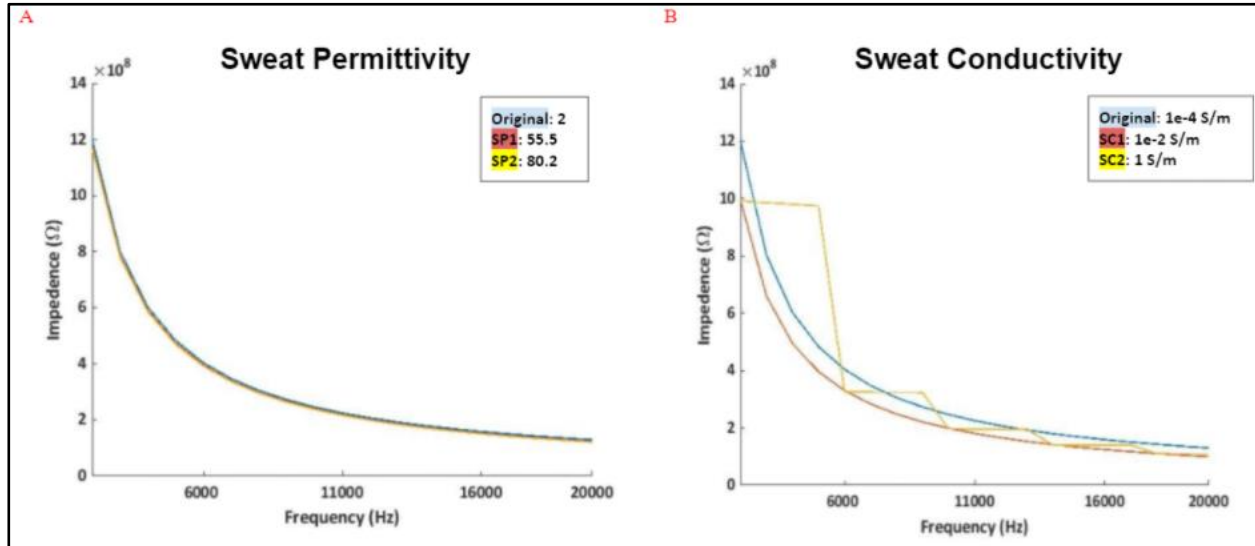


Figure 5.8: Impedance vs. frequency using sweat property values. (A) Sweat relative permittivity. (B) Sweat electrical conductivity.

For the epidermis conductivity and relative permittivity, the impedance vs. frequency graphs can be seen in Figure 5.9. As the relative permittivity of the epidermis increases, the impedance begins to decrease noticeably. This overall makes sense because the relative permittivity is how easily something can move through the material. The values for the epidermis relative permittivity are comparable to that of the sweat. The reason the same trend is not seen in the sweat relative permittivity graph could be due to the size. Since the pore is only 100 microns in radius, the distance is already so small that the permittivity is not making as much of an impact as the epidermis. The epidermis is 5 mm in diameter, thus the permittivity is going to show the hypothesized trend of a decrease in impedance. For the epidermis conductivity, the impedance decreases as the conductivity increases. This trend lines up with the sweat conductivity as well for the most part. The reason the graph remains consistent in characteristics is the lower conductivity values than that of sweat's.

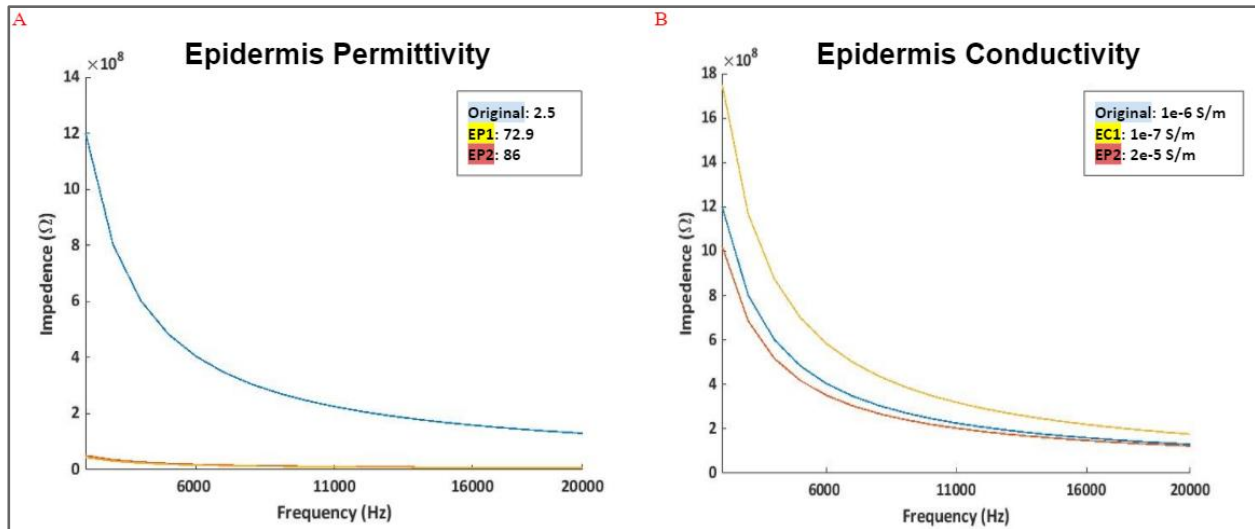


Figure 5.9: Impedance vs. frequency using epidermis property values. (A) Epidermis relative permittivity (B) Epidermis electrical conductivity.

For both sweat and the epidermis conductivity and relative permittivity, the COMSOL model was able to produce reasonable responses to the value changes. Once the size of the model is increased to a realistic size in the future, then we will be able to determine if those values such as in the sweat conductivity at 1 S/m was because of the scale.

5.2.4 Model Validation vs. Capacitor

To confirm that our model behaves as intended, we compared the data it produces to that of the Capacitor model from the COMSOL library. We changed the Capacitor model's conductivity and relative permittivity values to be the same as the values used in our epidermis model: epidermis electrical conductivity, 1×10^{-6} S/m, and a relative permittivity of 2.5. Then an impedance vs. frequency graph was achieved and can be seen in Figure 5.10 alongside the image of the capacitor from the COMSOL online source [18].

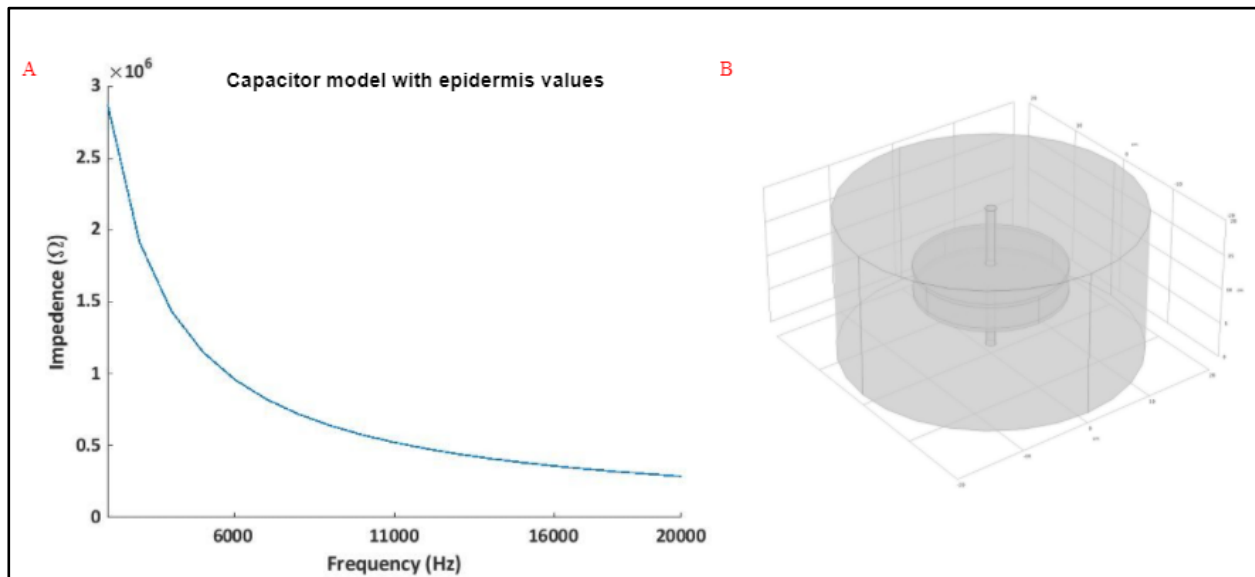


Figure 5.10: Capacitor model using epidermis property values. (A) Impedance vs. frequency graph produced using Capacitor model with epidermis relative permittivity and electrical conductivity values. (B) Capacitor model isometric view.

As mentioned earlier, this capacitor model has a critical difference compared to the skin phantom model we created. The capacitor model is contraplanar, where the electrodes are placed on the top and bottom of the flat cylinder. While ours is coplanar, the electrodes are on the same plane, in this case, the top of the model. A direct comparison of the impedance vs. frequency graph can be seen in Figure 5.11. From Figure 5.11B, the skin phantom model was tested with no sweat present at all, thus no sweat pooling. This is due to the capacitor model not having any pores or any form of liquid in the model. That way, the biggest differences are the electrode placement, size, and porosity. The impedance for the capacitor is about 3 magnitudes less than the skin phantom model. The capacitor model is 10 cm in diameter, while the skin phantom is only 5 mm in diameter. This comparison shows how the differences affect the impedance. A better demonstration of the comparison will occur, once the skin phantom is scaled up to size.

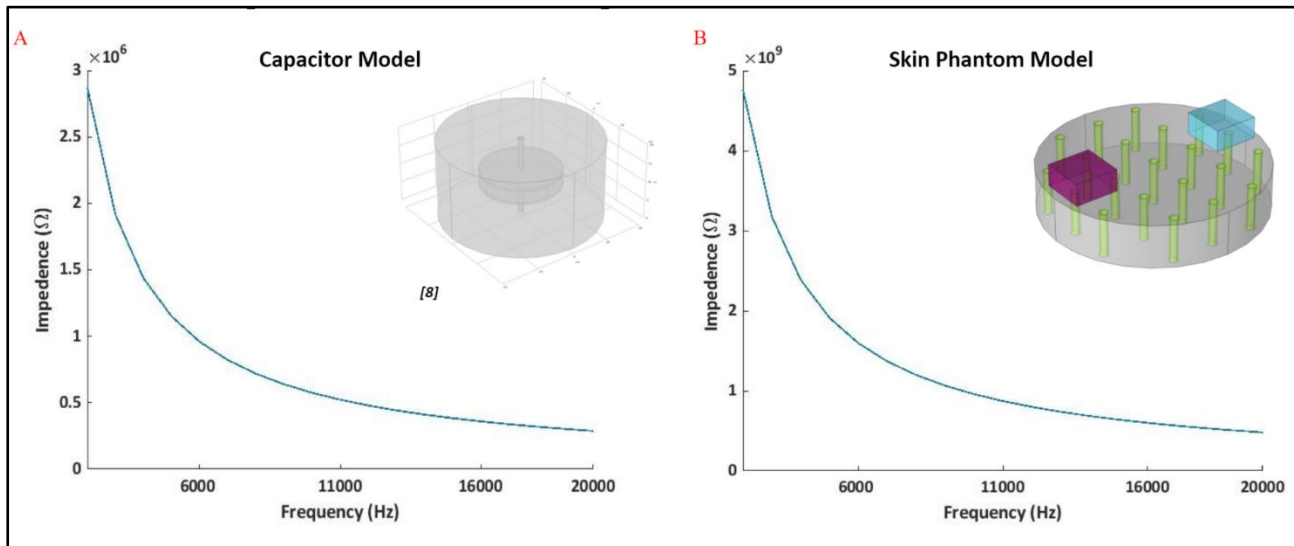


Figure 5.11: Impedance vs. frequency graphs with correlating models. Both models have the same conductivity and relative permittivity as the epidermis. (A) Capacitor, contraplanar electrodes [18]. (B) Skin phantom model, coplanar electrodes.

5.2.5 Model Validation vs. Real Skin

The final means of validating our model is comparing its data output to that produced by real human skin -- thus, determining whether the model fulfills our overall goal to accurately mimic skin's basic electrical properties. Figure 5.12 shows the impedance graphs of *in vivo* data compared to our simulation model's data. By comparing the graphs produced by our model to those produced from Proteus Digital Health's *in vivo* data, we found our model in agreement with the experimental skin results in terms of impedance behavior when exposed to a variety of frequencies and input voltages.

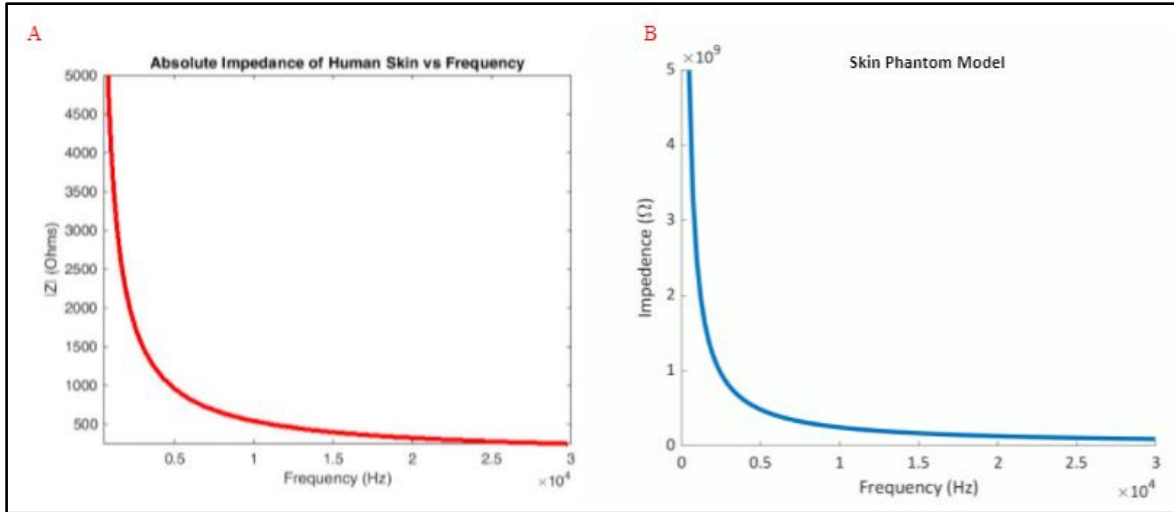


Figure 5.12: Impedance vs. frequency graphs from *in vivo* and our model.

(A) Proteus Digital Health, *in vivo* skin data [2]. (B) Our COMSOL skin phantom model.

Both plots demonstrate similar trend lines over a frequency range of near 0 to 30 kHz. The data produced by our model have a much larger impedance range than that of Proteus' data. This is largely due to differences in skin sample size. Our model is much smaller than the patch of skin tested by Proteus, with a diameter of 5 mm compared to Proteus' couple inches of skin. Another reason for the different impedance values is material differences: the data collected by Proteus uses real human skin and sweat which are much more intricate and variable than the materials used in our model. Since our model seeks to replicate the *general* electrical properties and behaviors of the skin, its validity still stands.

Chapter 6: Professional Engineering Standards and Realistic Constraints

6.1 Ethical Justification of Skin Phantoms

Ethical concerns and considerations are the primary motivation behind the development of this project, as concerns over current testing methods for biowearable devices led to research into alternative, more ethical options. Most times, companies have to test biowearable devices using animals, human volunteers, or skin samples from cadavers, with each method posing several challenges. Animals and human volunteers need to undergo screening for specific criteria to ensure population uniformity and testing standards are met, and the cost of animal testing is increasing by the year [33]. Cadavers prove to be particularly difficult to obtain for experimentation due to extensive regulations and limited supply which result in high demand and cost [33]. In addition, early-stage device testing on humans and animals can prove highly inaccurate or misleading due to individual variances and differences in human and animal skin properties.

Skin phantoms avoid putting living beings at risk while providing more accurate and consistent means of testing devices, as well as improved testing accessibility and resource management. Human and animal testing can result in unnecessary pain, injury, and even death. Producing medical devices that are safe and effective is vital to maintaining trust between a patient and a physician/company. Likewise, allowing a medical device or other biowearable to go to market without sufficient testing would be unethical as the devices could cause real harm. Thus, it is essential that such devices undergo proper, thorough testing, ideally using methods such as skin phantoms or computer model simulations for testing purposes to avoid causing unnecessary harm to any beings involved.

6.2 Health and Safety Implications

The health and safety implications of this project are all positive. The physical model we created for our educational kit uses simple, skin-contact-safe materials that can be handled with limited to no safety gear. The COMSOL model poses no health or safety concerns since it is entirely computer based. The long term health and safety implications of the COMSOL

model are that the simulation can provide better planning for a company creating a biowearable device. By being able to test via simulation, the manufacturer or company is better prepared to make any changes to make the device safer for future testing on live subjects and potential release to the public market.

6.3 Sustainability as a Constraint

As environmental concerns and failures continue to threaten the health of the planet, practicing sustainability is growing ever more important across all means of life, including within scientific research. To create a sustainable product, it must be one that is capable of maintaining a balance in its use of resources so that the resources are never depleted. With the educational kit model, the agar is plant based rather than animal- or synthetic-based, and the petri dishes used for layer molding can be cleaned and reused for future molds. Although the silicone used in the educational kit is synthetic, it is only needed in limited amounts, thus reducing its environmental impact. The COMSOL simulation is sustainable considering no materials are needed other than a basic computer, electrical power, and internet access (depending on whether the COMSOL program resides locally on your device or remotely on a shared server, such as the Engineering Design Center's remote access desktop program).

6.4 Civic Engagement and Compliance with Regulations

Our educational kit has a more direct and quick path to the community in the form of civic engagement because it is intentionally designed for public and private educational use. The very intent of the subsystem is to provide students a better understanding of skin biology and electrical engineering in the form of a low cost and resource pre-packaged kit. None of the materials used are hazardous or requires clearance to be used, so regulation is minimal to nonexistent for the educational kit. This is as intended, since the kit is geared towards students/persons from a range of ages.

Following further improvements and optimization, the COMSOL model can eventually be used as a program for companies to utilize to ensure safety of their devices, overall leading back to the community in the form of safer and more affordable devices. The latter aspect could come as a result of companies and manufacturers not having to spend as much money

on testing methods, thus lowering the overall cost of manufacturing and the resulting market price for customers. Seeing that the medical device industry is already heavily regulated, it is important that any devices or models continue to adhere to these constraints. With our COMSOL model, the intent is that companies could use it as an alternative to current methods for early-stage testing of biowearable devices, but the model should not replace all other forms of testing for a device. The model is simply meant to act as a replacement for methods that may be harmful (to animals, volunteers, etc.) or as a supplement to other early-stage testing to hopefully improve device success when it comes time for the biowearable device to be tested on live subjects. Any biowearable testing performed should remain compliant with federal regulations as appropriate. In the future, we hope that skin phantoms and simulation models could actually completely supplant some animal and human test trials, serving as its own stand alone testing method. Until technology improves, though, these skin phantoms and computer models can only serve as preliminary testing methods.

6.5 Manufacturability

For the educational kit, the manufacturability consists of a list of supplies needed depending on the amount of students participating in the lesson and where the supplies can be purchased from. Along with the list of the materials, an instruction packet is available for the instructor to utilize for planning the lesson in advance (see Appendix B). The COMSOL model can be uploaded to the internet as a digital file making it easy to distribute. Additionally, with all of the parameters being located under Global Parameters, our model makes it easier for the user to change what is needed for their testing purposes. Currently, each COMSOL model has an associated “README.txt” file that describes the general purpose of the model as well as how it differs from the other versions. An instruction packet can also be made to make the COMSOL model easier to follow and adjust as needed in the future.

6.6 Budget Constraints

For any research project, the provided budget acts as a constraint and thus, must be considered as such. For our project, we were given \$1,121.26 to purchase our anticipated equipment and materials. These funds were provided by the School of Engineering at Santa Clara University -- a detailed funding request is located in Appendix A.1. Our anticipated

total cost was \$1,121.26, however our actual expenses ended up being only \$390.37. A detailed spending list is located in Appendix A.2. The reason for our lowered costs is primarily due to changes in lab access as a result of changing county and school COVID-19 guidelines. These changes led us to pursue more affordable and accessible options such as our educational kit and COMSOL models; thus, we no longer needed most of the more expensive lab materials we initially requested.

6.7 Time Constraints

As with any long term project, we had to create a project work plan to ensure our project is completed in a timely manner, within the three quarters of the school year. Our initial timeline is available in Appendix C.1. Due to uncertainties regarding campus and lab access, and overall county restrictions, our project goals and projected timeline consequently changed. Our revised timeline is shown in Appendix C.2, along with notes indicating whether each goal was achieved within that time frame. Since we were ultimately unable to access or use the campus labs, we were unable to pursue a physical skin phantom model as we initially had intended. This was not determined to be inaccessible to our team until late fall quarter and early winter quarter 2020-2021. Much of our literature review was spent researching lab protocols and other related topics which ultimately proved rather unhelpful for project completion as we did not end up going into the lab, and instead were faced with having to learn and use an entirely new simulation program. In addition, due to county and state restrictions, our team was unable to meet up in person to work on the project or speak with our advisors. This proved especially challenging during COMSOL experimentation and file sharing using Google Drive and the engineering school's remote desktop access on separate devices, in separate locations. Such difficulties slowed the progress of model development and experimentation.

6.7.1 Model Constraints

Regarding our actual models, time constraints primarily reside in the setting of the agar and silicone in the educational kit and the kit's lifespan. The agar and silicone setting takes several days of preparation and the educational kit has a lifespan of about 2 weeks. However, this time constraint should not be worrisome for instructors since the kit's lesson plan only

asks for 2 to 3 days of preparation, depending on the lab meeting time. Likewise, the lesson is meant to be completed during a single lab period; but even if the lesson needed to continue into the following week's lab session, the model would still be functional at that point.

The COMSOL model run times are dependent on the user's computer and the type of CPU, GPU, and RAM. For our laptops with fairly decent hardware, most simulation runs only took a couple minutes. However, for a company testing biowearable devices this time constraint should not be applicable in the majority of cases as it is safe to assume that their company computers would meet the requirements to run COMSOL efficiently.

Chapter 7: Summary and Conclusion

7.1 Summary of Project Work

By the end of this project, we completed an educational kit that can be utilized at the highschool or entry level college courses and a foundational computer model for future simulation testing of biowearable devices. The process of the educational kit model has been flushed out and optimized with easy-to-follow instructions. The COMSOL model proved successful as a small-scale working model that demonstrates the electrical properties of the top most layer of skin. In addition, basic skin perspiration, electrode spacing, and the effects of conductivity and relative permittivity experiments were successfully explored for the means of our basic model.

7.2 Future Work

The physical model and computational models we have created have room for many future improvements. In their current states, they can serve as the foundational groundwork for future teams or students to further develop.

7.2.1 Educational Kit

All first year engineering students at Santa Clara University are required to take ENGR 1/1L: Introduction to Engineering Lecture & Lab, and each week revolves around a different discipline of engineering, including bioengineering. We noticed that the lab's bioengineering portion could be updated with our educational kit, which is interdisciplinary through the combination of bioengineering and electrical engineering. We have been in discussion with the course instructors and have created an instructional packet for the implementation of our physical model in the ENGR 1L coursework (Appendix A.3). While the budget may seem large right now, our engineering school already has many of the required pieces of equipment, which can be reused each quarter, bringing down the cost to only a few hundred dollars. If this were to be implemented, we would also want to create a "worksheet", which provides the students with information on the skin and instructs them to create deliverables for their instructors.

As previously mentioned, we have been experimenting with off-the-shelf products that can replace our silicone for the “epidermis” layer. By using two layers of microporous Transpore Surgical Tape, the methods would become much simpler and could be just as effective at allowing current to pass through. Future teams should consider experimenting more with these types of alternatives and compare its results with those of the porous silicone.

7.2.2 COMSOL Model

The educational kit can be expanded to incorporate different types of materials to compare models to see which best demonstrates the electrical properties of skin. The COMSOL model has a long road ahead. The baseline model can be built upon for the future. The first thing that needs to be done for the simulation model is upscaling to a realistic size and seeing if the experiments we have run still hold true. The next step would be adding fluid dynamics to show sweating over time, along with mechanical properties of the pore contracting during perspiration and movement of the epidermis surface. The model can then be expanded to have multiple layers to represent the entirety of the skin, each of which would have their own properties and physics features to manipulate and fine-tune.

7.3 Lessons Learned

One of the greatest lessons learned during this project is gaining the ability to remain vigilant amongst changes in plans and environments. The original plan for this year’s project was to continue optimizing last year’s, in lab, skin phantom. However, that main goal was unachievable due to not having access to the lab. We had to find a new strategy of how we could contribute to the end goal of creating a skin phantom that is more sustainable for people and the environment. Without the pandemic, it is very unlikely we would have learned how to use COMSOL from scratch to create a skin simulation model. It is even more unlikely an educational kit would have been created to implement in classrooms and show interdisciplinary skills of bioengineering and electrical engineering. Had we not been denied access to the lab, left unable to pursue the PDMS-carbon black skin phantom as we initially anticipated, we would have never created and explored these subsystems as we did.

References

- [1] S. Jary, “Fitness face off: Apple Watch vs. Fitbit,” Tech Advisor, 28-Mar-2021. [Online]. Available: <https://www.techadvisor.com/feature/wearable-tech/fitbit-vs-apple-watch-3612954/>
- [2] T. Henderson, J. Y. Lee, M. Placide, and K. Sutaria, “Developing a skin phantom for the testing of biowearables developing a skin phantom for the testing of biowearables,” *Interdisciplinary design senior theses*, no. 63, 2020. [Online]. Available: https://scholarcommons.scu.edu/idp_senior/63
- [3] B. W. Pogue and M. S. Patterson, “Review of tissue simulating phantoms for optical spectroscopy, imaging and dosimetry,” vol. 11, no. 4, pp. 041102–0411016, Sep. 2006, doi: 10.1117/1.2335429. [Online].
- [4] B. Godin and E. Touitou, “Transdermal skin delivery: predictions for humans from in vivo, ex vivo and animal models,” vol. 59, no. 11, pp. 1152–1161, Sep. 2007, doi: S0169-409X(07)00171-8 [pii].
- [5] M. C. Bach, “Still Human: A Call for Increased Focus on Ethical Standards in Cadaver Research,” vol. 28, no. 4, pp. 355–367, 2016, doi: 10.1007/s10730-016-9309-9. [Online].
- [6] N. A. Taylor and C. Machado-Moreira, “Regional variations in transepidermal water loss, eccrine sweat gland density, sweat secretion rates and electrolyte composition in resting and exercising humans,” vol. 2, no. 1, p. 4, 2013, doi: 10.1186/2046-7648-2-4. [Online]. Available: <https://pubmed.ncbi.nlm.nih.gov/23849497>
<https://www.ncbi.nlm.nih.gov/pmc/articles/PMC3710196/>
- [7] J. Garrett, and E. Fear, “Stable and flexible materials to mimic the dielectric properties of human soft tissues,” *IEEE Antennas and Wireless Propagation Letters*, vol. 13, pp. 599-602, 2014, doi:10.1109/LAWP.2014.2312925.
- [8] O. Pabst, Ø G. Martinsen, and L. Chua, “The non-linear electrical properties of human skin make it a generic memristor,” *Scientific Reports*, vol. 8, no. 1, p. 15806, 2018, doi:10.1038/s41598-018-34059-6.

- [9] L. B. Baker, “Sweating Rate and Sweat Sodium Concentration in Athletes: A Review of Methodology and Intra/Interindividual Variability,” vol. 47, pp. 111–128, 2017, doi: 10.1007/s40279-017-0691-5. [Online]. Available: <https://pubmed.ncbi.nlm.nih.gov/28332116>
<https://www.ncbi.nlm.nih.gov/pmc/articles/PMC5371639/>
- [10] S. Henkin, P. Sehl, and F. Meyer, “Sweat Rate and Electrolyte Concentration in Swimmers, Runners, and Nonathletes,” *International journal of sports physiology and performance*, vol. 5, pp. 359–66, 2010, doi: 10.1123/ijsp.5.3.359. [Online].
- [11] F. Flament et al., “Facial skin pores: a multiethnic study,” vol. 8, pp. 85–93, 2015, doi: 10.2147/CCID.S74401. [Online]. Available: <https://pubmed.ncbi.nlm.nih.gov/25733918>
<https://www.ncbi.nlm.nih.gov/pmc/articles/PMC4337418/>
- [12] A. Dąbrowska, G. Rotaru, S. Derler, F. Spano, M. Camenzind, S. Annaheim, and R. Rossi, “Materials used to simulate physical properties of human skin,” 2015. [Online]. Available: <https://onlinelibrary.wiley.com/doi/full/10.1111/srt.12235>
- [13] G. Canavese, S. Stassi, M. Stralla, C. Bignardi, and C. F. Pirri, “Stretchable and conformable metal–polymer piezoresistive hybrid system,” *Sensors and Actuators A: Physical*, vol. 186, pp. 191–197, 2012.
- [14] L. Hou, J. Hagen, X. Wang, I. Papautsky, R. Naik, N. Kelley-Loughnane, and J. Heikenfeld, “Artificial microfluidic skin for in vitro perspiration simulation and testing,” *Lab on a Chip*, vol. 13, no. 10, p. 1868, 2013.
- [15] M. Morales-Hurtado, X. Zeng, P. Gonzalez-Rodriguez, J. E. Ten Elshof, and E. van der Heide, “A new water absorbable mechanical Epidermal skin equivalent: The combination of hydrophobic PDMS and hydrophilic PVA hydrogel,” *Journal of the Mechanical Behavior of Biomedical Materials*, vol. 46, pp. 305–317, 2015.
- [16] A. Owda and A. Casson, “Electrical properties, accuracy, and multi-day performance of gelatine phantoms for electrophysiology,” 2020, doi: 10.1101/2020.05.30.125070. [Online].

- [17] L. Davies, “A Cellular Model of the Electrical Characteristics of Skin,” *University of Southampton*, Sept. 2018. [Online]. Available: eprints.soton.ac.uk/id/eprint/423466.
- [18] COMSOL, “Frequency Domain Modeling of a Capacitor”. [Online]. Available: <https://www.comsol.com/model/frequency-domain-modeling-of-a-capacitor-12693>
- [19] “Pouring Agar Plates”, 2021, [Online]. Available: <https://bio.libretexts.org/@go/page/36761>
- [20] S. Iverson, T. Eidenschink, T. Dale, and D. Broman, “Synthetic Tissue Phantom for Medical Evaluation,” 2017 [Online]. Available: <https://patents.justia.com/patent/20180075777>
- [21] “Dry Etching and Wet Etching.” [Online]. Available: <https://www.thierry-corp.com/plasma-knowledgebase/dry-etching-and-wet-etching>
- [22] B. Hoex, “Etching,” *PV Manufacturing*. [Online]. Available: <https://pv-manufacturing.org/etching/>
- [23] “Speciality Crystalline White Sugars,” British Sugar, Peterborough, May 5. [Online]. Available: <https://www.britishsugar.co.uk/perch/resources/speciality-crystalline-white-sugars.pdf>
- [24] V. Solano, Immobilization of Gold and Silver on a Biocompatible Porous Silicone Matrix to Obtain Hybrid Nanostructures. 2018. [Online]. Available: https://www.researchgate.net/publication/322724563_Immobilization_of_Gold_and_Silver_on_a_Biocompatible_Porous_Silicone_Matrix_to_Obtain_Hybrid_Nanostructures
- [25] D. Zhu, S. Handschuh-Wang, and X. Zhou, “Recent progress in fabrication and application of polydimethylsiloxane sponges,” vol. 5, no. 32, pp. 16467–16497, 2017, doi: 10.1039/C7TA04577H. [Online]. Available: <http://dx.doi.org/10.1039/C7TA04577H>
- [26] “How to Differentiate 3M Surgical Tapes ,” 2015. [Online]. Available: <https://multimedia.3m.com/mws/media/1074994O/surgical-tape-tool-1504-01038b.pdf>

- [27] Coin Cell Battery Pack. [Online]. Available: <https://www.youtube.com/watch?v=IWQiQ8VF7uo&t=54s>
- [28] COMSOL, “System Requirements: COMSOL Server™ Version 5.5”. [Online]. Available: <https://www.comsol.com/system-requirements/55/server>
- [29] “Basics of Electrochemical Impedance Spectroscopy.” [Online]. Available: <https://www.gamry.com/application-notes/EIS/basics-of-electrochemical-impedance-spectroscopy/>
- [30] A. R. El-Damak, S. Thorson, and E. C. Fear, “Study of the Dielectric Properties of Artificial Sweat Mixtures at Microwave Frequencies,” *Biosensors*, vol. 10, no. 6, p. 62, 2020, doi: 10.3390/bios10060062. [Online]. Available: <https://www.mdpi.com/2079-6374/10/6/62/htm>
- [31] C. R. Nave, “Use of Complex Impedance,” *HyperPhysics*, 2016. [Online]. Available: <http://hyperphysics.phy-astr.gsu.edu/hbase/electric/impcom.html#c1>. [Accessed: 22-Apr-2021].
- [32] M. Patterson, S. Galloway, and M. Nimmo, “Variations in regional sweat composition in normal human males,” vol. 85, no. 6, pp. 869–875, 2000.
- [33] M. N. Helmus and B. Sall, “Biomaterials in the design and reliability of medical devices,” in *Madame Curie Bioscience Database [Internet]*., Austin, TX: Landes Bioscience, 2003.

Appendix A: Budget and Actual Spending

A.1: Proposed Budget (if lab were accessible)

| | Item | Unit Size | Quantity | Cost |
|--|---|----------------|------------------------|-------------------|
| Electrical | Metal Electrode: Set of 11 | 11 | 1 | \$38.00 |
| | Coil Shim Stock – 316 Stainless Steel (316-003-6-50) | 1 | 1 | \$40.57 |
| Biological/ Chemical | Carbon Black - Vulcan XC 72, 50g Bottle | 1 | 1 | \$60.00 |
| | Carbon Black - Vulcan XC 72R, 50g Bottle | 1 | 1 | \$60.00 |
| | Sodium Chloride, 0.9% w/v, Standards and Solutions, Bottle, 500mL | 1 | 1 | \$42.53 |
| | Sylgard 184 (PDMS) | 1 | 2 | \$268.90 |
| | Artificial Sweat, ISO-3160-2 1L | 1 | 1 | \$144.70 |
| | Fumasep FAS-30 (size 20x30) | 5 | 5 | \$99.93 |
| | Petri Dish w/ Pipettes | 20 | 1 | \$11.99 |
| | 10mL Luer Lock Syringe | 100 | 1 | \$14.99 |
| | 20gax0.5" Dispensing Tip | 50 | 1 | \$15.99 |
| | 21gax0.5" Dispensing Tips | 50 | 1 | \$15.99 |
| | Tygon Microbore tubing | 1 | 1 | \$61.00 |
| | Thermometer (humidity) | 1 | 1 | \$10.99 |
| | Miscellaneous | Nitrile gloves | 1 | 1 |
| KN95 Masks | | 50 | 1 | \$79.99 |
| Plastic bin | | 1 | 1 | \$17.55 |
| Replacement Blades for Cricut Machines | | 2 | 1 | \$9.59 |
| Deep Cut Blades for Cricut Explore Air 2, 60° Cutting with Anti Lost Bag & Storage Container | | 10 | 1 | \$8.99 |
| | | | TOTAL | \$1,028.68 |
| | | | Est. Tax | \$92.58 |
| | | | TOTAL REQUESTED | \$1,121.26 |

A.2: Purchase Record

| | Item | Unit Size | Quantity | Cost |
|---------------------------------|--|-----------|----------|-----------------|
| Electrical | Alligator Clips | 2 | 1 | \$7.99 |
| | 3V Lithium Coin Battery | 6 | 2 | \$17.10 |
| | Digital Multimeter | 1 | 3 | \$77.97 |
| | Disposable ECG Diagnostic Tab Electrodes | 500 | 1 | \$22.99 |
| | Conductive Gel | 1 | 1 | \$5.05 |
| Biological/ Chemical | Morton Salt | 3 | 1 | \$11.88 |
| | Miraclekoo Silicone Mold Making Kit Liquid Silicone Rubber Clear Mold | 3 | 1 | \$41.97 |
| | Agar, 6 g, dehydrated | 1 | 5 | \$30.15 |
| | Agar, nutrient, 100 g, dehydrated | 1 | 1 | \$29.95 |
| | Square Petri Dishes | 10 | 1 | \$12.59 |
| | Ecoflex 00-30 Super Soft Platinum Silicone | 1 | 1 | \$39.91 |
| Miscellaneous | Premium Filter Paper | 100 | 1 | \$8.89 |
| | Digital Weighing Scale | 1 | 3 | \$44.97 |
| | Turn-Table for Paint Spraying | 1 | 1 | \$15.96 |
| | 200micron Mesh Bag | 1 | 3 | \$6.99 |
| | Caster Sugar | 1 | 1 | \$11.99 |
| | Transpore Surgical Tape | 1 | 12 | \$13.01 |
| TOTAL SPENT | | | | \$399.36 |

Appendix B: Engineering 1 Lab Instruction Packet



ENGR 1L Instruction Packet

Skin Phantom - Bioengineering Component

Ruby Karimjee, Jordan Spice, Brooke Fitzwilson
April 2021

Objectives

Students will:

1. Learn how to work with biological components to create a 2-layered model that simulates the elastomeric and conductive properties of skin.
2. Understand how to build an electrical circuit in series.
3. Learn how to take accurate current measurements using ECG electrodes and Digital Multimeters.

Lab: Week 1

Preparation of Silicone

This portion should be done by the students one week beforehand and kept at room temperature conditions afterwards.

1. Line the surface of your turn-table with plastic. On top of it, place half of a petri dish, open-side down.
2. Tare an empty filter paper on your weighing scale to make sure it is set to “grams”. Weigh 5 grams of caster sugar and 5 grams of salt on the same paper.
3. Set the sugar and salt to the side, and tare an empty plastic cup on your weighing scale. Fill the plastic cup with 10 mL of part A and 10 mL of part B.
4. Set a timer for 5 minutes and immediately begin stirring the silicone with a plastic knife until the timer ends. Use a folding motion (like folding cake batter) and make sure to work in any material that may be on the sides of the cup. If you get tired, pass it off to a partner for the remainder of the time.
5. Immediately after the timer ends, pour the silicone onto the center of your petri dish. You will be turning the table in a fast-motion for at least 5 minutes and should see excess silicone dripping off the edges (see Figure 1)
6. Do not disturb the silicone and carefully place this setup at the location given by your instructor. You will be using your cured silicone during the next lab session.



TA: 2 Days Before Lab 2

Making Silicone Porous

You will now be leaching the sugar out of your silicone in order to make micropores in your “epidermis”.

1. Carefully peel the edges of the silicone off of the petri dish before peeling off the whole layer. Be careful not to tear the layer.
2. Place the silicone in a thermos and fill with boiling water. Seal tightly and not open until the next lab period.

Lab: Week 2

Preparation of Porous Silicone

1. Ask a TA for your team's thermos, which has your silicone layer inside.
2. Drain the water out of your thermos and carefully place your silicone layer onto a paper towel to pat dry. It should feel grainy, indicating that sugar has "leached" out.

Preparation of Agar

1. Wrap the inside of the petri dish in plastic wrap. Use a pencil or narrow object to flatten the plastic wrap, trying to minimize any air bubbles that may form. Press the plastic into the four corners of the dish to make sure the plastic is inside each crevice.
2. Making the silicone layer

- a. Agar base:

- i. Tare an empty container and use it to measure 75mL (or 75 grams) of water on the weighing scale in a microwave-safe container.
- ii. Make sure your balance is set to measure "grams" and tare an empty filter paper. Use it to measure 0.075 grams of salt. This creates 1% NaCl solution (0.075 g. of NaCl in 75 mL of water)
- iii. Use another filter paper, tare, and measure 3 grams of dehydrated agar. Add this to the NaCl water and stir with a glass stirring rod. This creates 4% agar (3 g. of dehydrated agar in 75 mL of water).
- iv. Stir the mixture and microwave for 30 seconds straight. Take it out and stir again before microwaving in 10 second intervals. At each interval, check if the mixture is boiling and stir. Once boiling (bubbles form), remove and stir once again to fully dissolve the agar.
- v. Move quickly to pour the mixture into the plastic-lined petri dish. Tap the sides of the dish to remove any bubbles after pouring (Figure 2).
- vi. Let this sit for 1 hour. It should become the consistency of Jello.



Figure 2: Measure Salt on Filter Paper

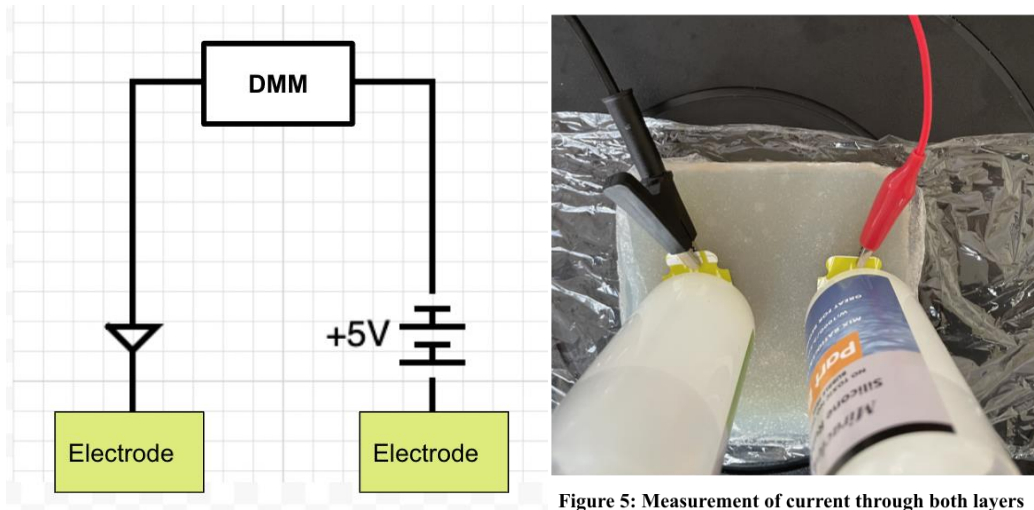
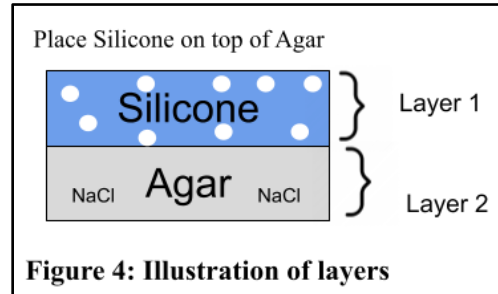
3. While waiting for the agar, set up your battery and digital multimeter.

- a. The battery has a "+" side and a "-" side. Use a hot glue gun to attach the end of the red wire to the "+" side of your battery, making sure the wire is in direct contact with the battery under the glue. Let this cool for ~3 minutes. Repeat to connect the end of the black wire to the "-" side of the battery and cool.
- b. The Digital Multimeter (DMM) has a red probe that connects to the "VΩmA" slot and a black probe that connects to the "COM" (ground) slot. Insert these probes into the DMM.



Figure 3: Agar Layer in Pre-Cooling Period

- c. Set the DMM dial to “V” to measure the voltage from the battery. Readings should be around 2.9-3 V. If not, your wire may not be in close enough contact with your battery, so you must remove the glue and reseal the wires. Contact a TA if you believe your battery or DMM are faulty.
2. Once your agar is dry, create your circuit.
- Place your dry silicone layer on top of the Agar (Figure 4).
 - Place electrodes on either ends of the skin phantom on top of the silicone. Use a ruler to make sure they are both 0.5mm from the edge.
 - Create a circuit with the battery and phantom in series. Connect the red probe alligator clip from the DMM to the red wire of the battery. Connect the black wire of the battery to an alligator clip, whose opposite side will be connected to an electrode. The other electrode will be connected directly to the ground/COM of the DMM. (Figure 5)
 - Switch the DMM dial to “uA” or “mA” to measure the current flowing through your skin phantom.



Material Purchase Links

Estimated cost for 30 students divided into 10 groups of three

| ITEM | QUANTITY | DESCRIPTION | COST |
|-------------------------|----------|-------------------------------|-----------------|
| Lithium Coin Battery | 2 | 3V, Pack of 6 | \$21.80 |
| Digital Multimeter | 10 | N/A | \$119.80 |
| ECG Electrodes | 1 | Pack of 500 | \$23.57 |
| Spectra 360 Gel | 3 | N/A | \$15.45 |
| Alligator Clips | 2 | Black and red, Pack of 5 | \$14.50 |
| Weighing Scale | 5 | Grams and ounces | \$25.76 |
| Filter Paper | 2 | Pack of 100 | \$17.78 |
| Non-Iodized Salt | 1 | Pack of 3 | \$10.13 |
| Caster sugar | 2 | N/A | \$23.98 |
| Dehydrated Agar | 1 | 100g | \$30.00 |
| Glass bottle | 2 | Pack of 12, Microwave-safe | \$45.98 |
| Insulated Thermos | 3 | Pack of 4s | \$86.64 |
| Turn-table | 3 | N/A | \$32.97 |
| Stirring rod | 2 | Pack of 12 | \$17.98 |
| Liquid Silicone Rubber | 2 | 28 oz | \$70.00 |
| Square Petri Dishes | 5 | Pack of 10 | \$62.95 |
| Plastic Wrap | 1 | N/A | \$4.35 |
| Disposable Plastic Cups | 2 | Pack of 30 | \$2.99 |
| Plastic Knives | 1 | Pack of 50 | \$5.99 |
| | | Total: | \$632.62 |

Appendix C: Project Timeline

C.1: Original Projected Timeline

| Quarter | Goal |
|-------------|--|
| Fall 2020 | Complete Literature Research |
| | Determine Parameters & Materials to Test |
| | Create Proposed Budget |
| | Get Lab Access |
| | Learn Lab Protocols and Fabrications |
| Winter 2021 | Start COMSOL Model |
| | Begin Lab Fabrication Training |
| | Preliminary Model Fabrication |
| | Finalize Parameters to Test |
| Spring 2021 | Lab Work on Device Composition |
| | Continue COMSOL Simulation Tests |
| | Consolidate Data |

C.2: Actual Timeline Due to Campus Closures/Lab Access

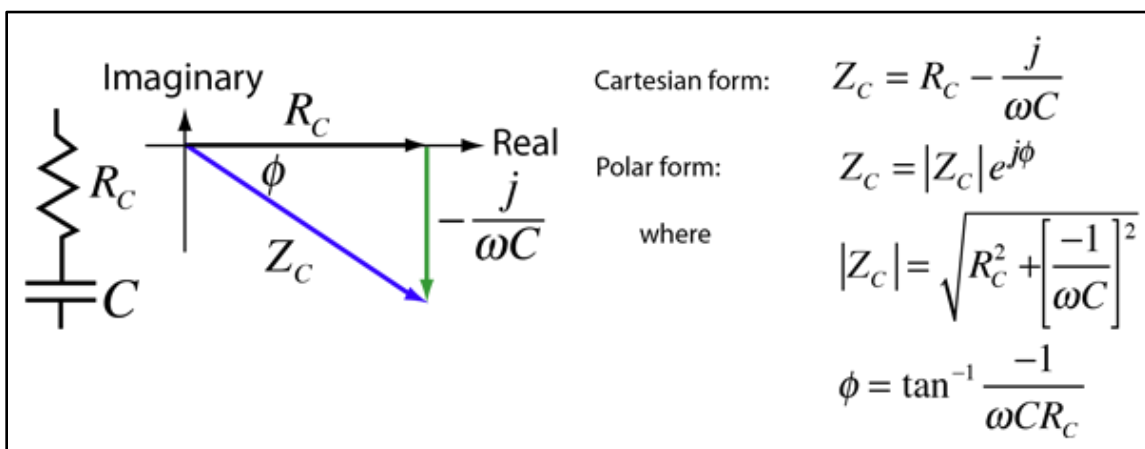
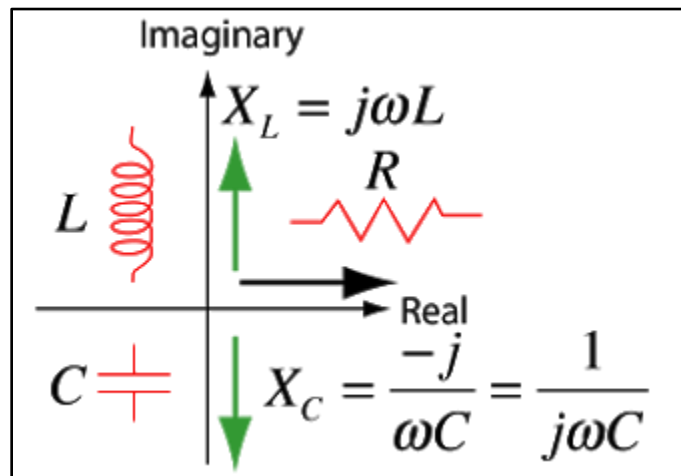
| Quarter | Goal | Achieved |
|-------------|---|-----------|
| Fall 2020 | Complete Research | Yes |
| | Begin COMSOL Model | Delayed |
| | Create Proposed Budget | Yes |
| | Get Lab Access | Denied |
| Winter 2021 | Create COMSOL Model | Continued |
| | Get Lab Access | Denied |
| | Run Physical Model Experiments | Yes |
| | Begin Proposing Educational Kit to ENGR 1 Lab | Yes |
| | Continue Literature Research | Yes |
| Spring 2021 | Wrap up COMSOL Simulations | Yes |
| | Wrap up Physical Model Experiments | Yes |
| | Present in Senior Design Conference | Yes |
| | Complete Senior Design Thesis | Yes |

Appendix D: COMSOL Equations

D.1: Current Conversion Equations

$$\begin{aligned} \nabla \mathbf{J} &= \mathbf{Q}_{jv} \\ \mathbf{J} &= \sigma \mathbf{E} + j\omega \mathbf{D} + \mathbf{J}_e \\ \mathbf{E} &= -\nabla V \end{aligned}$$

D.2: Complex Impedance for RC Circuit [31].



Appendix E: MATLAB Program

E.1: Example Text File Export from COMSOL

Text File Name: r100h50_orig.txt

```
COMSOL File Name
% Model: 5_04_SPC_SweatPool_PDMSx2.mph
% Version: COMSOL 5.5.0.359
% Date: May 4 2021, 13:56
% Dimension: 1
% Nodes: 19
% Expressions: 1
% Description: Global
% X Height
2000 8.331069449383359E-10
3000 1.2476115798563165E-9
4000 1.659896147981642E-9
5000 2.069245006698629E-9
6000 2.4751124724489284E-9
7000 2.877053952622121E-9
8000 3.274732079549217E-9
9000 3.6679147978018886E-9
10000 4.056468714907725E-9
11000 4.440348955487639E-9
12000 4.819586811034756E-9
13000 5.19427637926999E-9
14000 5.5645611915424E-9
15000 5.930621584783389E-9
16000 6.292663327956103E-9
17000 6.650907790854419E-9
18000 7.005583761707948E-9
19000 7.356920884821233E-9
20000 7.705144598395438E-9
```

Header

Frequency

Admittance

E.2: Pseudocode

- ① Find .txt file according to ^{file} name input
 - ② Extract Admittance & Frequency data from file
 - ③ Calculate Impedance from Admittance
 - ④ Plot Impedance vs. Frequency
 - ↳ Depending on experiment series, either plot multiple lines on one figure for different variables or one line per plot
 - ↳ ^{Plot} Lines can be comparing different Sweat Pool Radii or Height, or another variable like conductivity values
 - ⑤ Loop through Plot Creation until all data has been plotted
- * All plots are auto-labeled upon creation (legends, axes, titles, etc.)

E.3: Example Main Script (Commented)

IMPEDANCE VS. FREQUENCY CALC & PLOT

Skin Phantom for Biowearable Devices -- Brooke Fitzwilson, Ruby Karimjee, & Jordan Spice -- Santa Clara University, Bioengineering Senior Design 2020-2021

```
% This code extracts the data exported by our COMSOL model and plots
the desired data as specified below.

clear all; clc; close all;

%Variable strings
h = {'5', '50', '250', '500'}; %sweat pool heights
rad = {'100', '150', '200', '250'}; %sweat pool radii
test = {'wp0', 'wp1', 'wp2', 'pp0', 'pp1', 'pp2'}; %variable
%test: 0=original 1=lower 2=higher; wp (water permittivity)
tbase = 'PDMSx2: Sweat Pool R'; lgnd = cell(size(rad)); %title/legend
for g = 1:length(rad) %generate legend var from var chosen
    lgnd{g} = strcat(rad{g}, ' \mum');
end
zoomcheck = 1; %do you want a zoomed in portion of the graph

%Plot
for i = 1:length(rad) %dif fig for each radii
    for ii = 1:length(test) %dif line for each test variable
        %get data from txt
        [zImp, Hz] = comsolextraction(rad{i}, test{ii}, h);
        figure('Position', [785, 275, 690, 500]); hold on;
        for j = 1:length(rad)
            %plot for each dataset
            plot(Hz{j}, zImp{j}, 'LineWidth', 1.25);
        end
        xlabel('Frequency (Hz)'); ylabel('Impedence (\Omega)');
        %creates automatic title based on var used
        title(strcat(tbase, rad{i}, ' [', test{ii}, ']'));
        legend(lgnd{1:j}, 'Location', 'NorthEast');

        set(gca, 'FontWeight', 'bold', 'FontSize', 12, 'FontName', 'Calibri', 'Units', ...
            'normalized', 'XTick', [6e3, 11e3, 16e3, 20e3], 'XTickLabel',
            [6e3, 11e3, 16e3, 20e3])
        if zoomcheck == 1 %create zoom-in view (inside current fig)
            axes('position', [.4 .44 .32 .32], 'nextplot', 'add');
            box on %outlines zoomed area
            for k = 1:length(rad)
                %find impedance values for specified range of Hz
                iZoom = (Hz{k} < 6100) & (Hz{k} > 3900);
                %plot lines
                plot(Hz{k}(iZoom), zImp{k}(iZoom), 'LineWidth', 1.1);
            end
            axis tight;
        end
        hold off;
    end
end
end
```

E.4: Example Local Functions (Commented)

E.4.1: comsolextraction()

```
function [z, f, s] = comsolextraction(rad,suffix,hlist)
###INPUT: ([R]',',[suffix]',',[H]{''})
% Radius = string; suffix = string, hlist = cell matrix of str
###OUTPUT: impedance z (Ohms), frequency f (Hz), admittance s (S)

%preallocating variables
z = cell(size(hlist)); f = cell(size(z)); s = cell(size(z));
for i = 1:length(hlist)
    %creating filename variable based on data provided
    filename = strcat('r',rad,'h',hlist{i},'_',suffix,'.txt');
    %call local function 'getdata' to read .txt file
    [zraw, fraw, sraw] = getdata(filename);
    %store data from .txt file in cell matrices for output
    z{i} = zraw; f{i} = fraw; s{i} = sraw;
    %clear raw data variables for next loop iteration
    clear zraw fraw sraw
end
end
```

E.4.2: getdata()

```
function [Z, Hz, S] = getdata(title)
    %check if filename exists; if not, stop & display error
    assert(exist(title,'file') == 2,...
        '<!><!> FILE ''%s'' NOT FOUND <!><!>',title);

    %open COMSOL text file & scan for data values
    fid=fopen(title);
    %skips 8 headerlines of .txt file
    txt=textscan(fid,'%f %f','headerlines',8);
    fclose(fid); %close .txt file
    x=txt{1}; %frequency values
    y=txt{2}; %admittance values

    %remove any potential repeated sets of data
    stop = 0;
    for i = 2:length(x)
        if y(i) == y(1)
            stop = i;
            break
        end
    end

    %assign data sets to correct variables
    if stop > 0
        Hz = x(1:stop-1);
        S = y(1:stop-1);
        clear stop
    else
        Hz = x';
        S = y;
    end

    Z = impedance(S); %use local fxn to calculate impedance
end
```

E.4.3: impedance()

```
function Z = impedance(S)
    %Calculates the impedance using admittance values
    %INPUT = admittance S; OUTPUT = impedance Z
    Z = 1./S;
end
```